

Missing Puzzle Pieces in the Performance Landscape of the Quantum Approximate Optimization Algorithm

Elisabeth Wybo^{1,*} and Martin Leib^{1,†}

¹*IQM, Georg-Brauchle-Ring 23-25, 80992 München, Germany*

We consider the maximum cut and maximum independent set problems on random regular graphs, and calculate the energy densities achieved by QAOA for high regularities up to $d = 100$. Such an analysis is possible because the reverse causal cones of the operators in the Hamiltonian are associated with tree subgraphs, for which efficient classical contraction schemes can be developed. We combine the QAOA analysis with state-of-the-art upper bounds on optimality for both problems. This yields novel and better bounds on the approximation ratios achieved by QAOA for large problem sizes. We show that the approximation ratios achieved by QAOA improve as the graph regularity increases for the maximum cut problem. However, QAOA exhibits the opposite behavior for the maximum independent set problem, i.e. the approximation ratios decrease with increasing regularity. This phenomenon is explainable by the overlap gap property for large d , which restricts local algorithms (like QAOA) from reaching near-optimal solutions with high probability. In addition, we use the QAOA parameters determined on the tree subgraphs for small graph instances, and in that way outperform classical algorithms like Goemans-Williamson for the maximum cut problem and minimal greedy for the maximum independent set problem. In this way we circumvent the parameter optimization problem and are able to derive bounds on the expected approximation ratios.

I. INTRODUCTION

The advent of quantum computing promises advantage over classical computing in areas as diverse as quantum simulation [1–3], machine learning [4–7] and optimization [8, 9]. To unequivocally profit from this however, fault tolerant operation of quantum computers is needed. In the current era of Noisy Intermediate Scale Quantum (NISQ) devices [10], it is not possible to run the deep quantum algorithms equipped with proofs of quantum advantage. Therefore, a new research topic of quantum heuristics with substantially reduced number of required gate operations is currently flourishing. The reduced number of gates for these heuristics comes typically at the cost of unclear prospects for quantum advantage caused by a lack of techniques for their complexity analysis. Compared to other quantum algorithms for the NISQ era, there is however already a lot known about performance and time-to-solution for the Quantum Approximate Optimization Algorithm (QAOA) [11–17] which the current work is adding a missing puzzle piece to.

Two basic insights have enabled analytical investigations of the average performance of the QAOA: First, the fact that the expected performance of QAOA is the sum over terms which are only affected by a subset of gates, called the Reverse Causal Cone (RCC), which is limited by the number of layers in the QAOA circuit and not the actual problem size. Second, the focus on either all-to-all or random regular problem graphs. Random d -regular graphs have the convenient property that the p -local environments of the nodes and edges, are asymptotically (with growing number of graph nodes N) trees. This is because the probability of having small loops vanishes [18]. Consequentially the topology of the qubits involved in a single RCC of QAOA is also, with high probability a tree. Therefore, it follows that the asymptotic performance of QAOA with depth p , is fully determined by its performance on those tree structures [11, 19], which are particularly convenient to calculate classically. These locality arguments have already been explored in the original QAOA paper for 3-regular graphs [11]. Additionally, it was also possible to calculate optimal, instance- and problem size-independent, parameters thereby creating a optimization loop free variation of QAOA termed ‘tree QAOA’ [20–23].

With the help of the above described techniques it was possible to show that QAOA outperforms the classical guarantee of the Goemans-Williamson (GW) algorithm for the Maximum Cut (MaxCut) problem, if p is large enough [24–29]. The GW algorithm [30] is the optimal classical approximate algorithm for this problem with a performance guarantee, assuming that the unique games conjecture is true [31]. It should be noted however, that there are classical algorithms without a performance guarantee, that are on average better than GW [29, 32–34]. For the MaxCut problem, the asymptotic QAOA angles have been determined explicitly for the smallest p [11, 16, 25, 28],

* elisabeth.wybo@meetiqm.com

† martin.leib@meetiqm.com

either using numerical contraction [21, 26], or by evaluating recursive formulas that describe the contraction sequence analytically [19, 35, 36]. The numerical approach of Refs. [21, 26] is limited to fairly small regularities. On the other hand, in the approach of Ref. [19] the regularity does not enter in the complexity of the evaluation of the variational energy. The tree angles have been evaluated up to $p = 11$ for MaxCut on 3-regular graphs [26]. This also implies that the asymptotic performance of QAOA on this problem is known explicitly up to depth $p = 11$. However, the performance scaling with p is not formally known. Summarizing, it can be said that fixed depth QAOA exhibits a constant, non-vanishing performance as function of the problem size N , which can also be extended to Sherrington-Kirkpatrick models on all-to-all connected problem graphs.

In contrast to this, it has been explicitly shown that constant depth QAOA has strong sub-optimal performance for the Maximum Independent Set (MIS) problem [37, 38]. Indeed, the minimal requirement to find solutions close to the optimum is ‘to see the whole graph’, thus that $p \gtrsim \log(N)$, making QAOA an algorithm with increasing sample complexity. This observation of widely differing algorithm performance for two NP-hard problem classes, MaxCut and MIS, is not restricted only to quantum algorithms but also extends to classical algorithm performance.

A recent, very successful attempt at explaining this phenomenon employs the so-called Overlap Gap Property (OGP) that can be linked to algorithmic hardness. Problems that do have an OGP, like MIS, possess an intricate property associated to the clustering of good solutions [39–42]. Solutions that are close to optimality for instances which possess OGP are either very similar or very different, implying that there are remote clusters of good solutions in the state space.

It can be shown that the existence of an OGP implies that there is an a priori gap between what p -local algorithms (like QAOA) can possibly achieve, and optimality. In contrast to this, for problems without OGP [43–45], we may be able to find a p -local algorithm that produces solutions $(1 - \epsilon)$ close to optimality with high probability. The statement ‘with high probability’ is important, and implies that there is no guarantee that such a good $(1 - \epsilon)$ approximation can be always reached, as otherwise complexity theoretic statements like the unique games conjecture [31], and therefore also $P \neq NP$, would collapse. For MaxCut on regular graphs, such an approximate $(1 - \epsilon)$ classical algorithm has been proposed in Ref. [34], with the remaining condition that ϵ cannot be made arbitrary small $d > O(1/\epsilon)$ yet. The largely differing behaviour for problems with and without OGP is greatly enhanced for random regular graphs in the regime of high regularity. This regime has been treated with QAOA for MaxCut with less stringent bounds on optimality which in the end suggest qualitatively wrong results [26]. For the MIS problem this regime has not been explicitly investigated yet with QAOA to the best of our knowledge.

In this work we fill these gaps by first extending the technique of the recursive formula of Ref. [19] to MIS, enabling performance calculations in the high regularity regime. We start by showing how to treat the MaxCut problem and the MIS problem on equal footing using the language of Ising models with local fields. With a range of numerical improvements in evaluating the recursive formula, we are able to determine tree QAOA performance for Ising models with local fields $H = \sum_{ij \in E} Z_i Z_j + h \sum_{i \in V}$ for $N \rightarrow \infty$ on graphs with regularities up to $d = 100$.

In addition, we combine these results with state-of-art upper bounds on optimality. For MaxCut, upper bounds on the cut fraction in the asymptotic limit for d -regular graphs have been determined in Refs. [46, 47]. For MIS, upper bounds on the independence ratio in the asymptotic limit for d -regular graphs have been determined in Refs. [48, 49]. Taking into account these findings yields higher performance guarantees for QAOA in the asymptotic limit than previously assumed, and changes insights on the qualitative behaviour in the large d regime. This is mainly relevant for MaxCut: for instance in Ref. [26] it is observed that asymptotic tree QAOA outperforms the GW guarantee at $p \geq 11$. However, by combining the QAOA performance with state-of-the-art bounds on optimality, it can be realized that this actually already happens when $p \geq 4$ for $N \rightarrow \infty$. This observation is only true in the large N limit, but however gives hope that an effective quantum utility regime can be reached in the near term for this problem, with a local quantum algorithm.

Combining the better bounds with the extended method of the recursive formula, we are in the end able to show that the manifestly different problem hardness of MaxCut and MIS for larger graph regularities results in a performance difference of QAOA. While for MaxCut the approximation ratios achieved by fixed- p QAOA are increasing with d , they are decreasing for MIS. This reflects the finding that the MIS problem has an OGP regime for large d [50]. Despite these findings, there is still hope that with a quantum algorithm breaking locality, i.e. for QAOA with $p > O(\log(N))$, good performances (potentially even inside the OGP regime) can still be achieved in polynomial-time on a quantum computer. In addition, there is also future hope that hybrid approaches can provide such good performances in overall polynomial time [51–57].

Our paper is organized as follows: In Sec. II, we introduce the QAOA algorithm and discuss its $N \rightarrow \infty$ limit for regular graphs, the ‘tree QAOA’. In Sec. III, we discuss the MaxCut and MIS problems and show how they can be unified as Ising models. Here, we also define the performance metrics that we will measure on the QAOA ansatz state in order to get the expected solution quality of the sampled solutions. In Sec. IV, we briefly review the concept of Overlap Gap Property and local algorithms, and provide a short overview about the different hardness regimes of the two problems, and the implications for QAOA. In Sec. V, we present and discuss our results. The main result of our

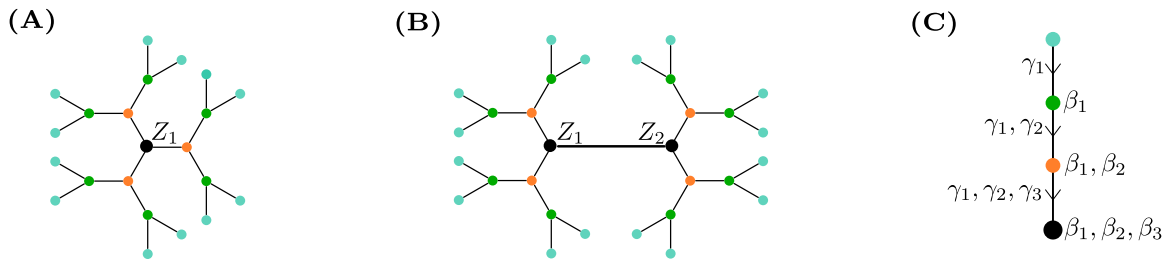


FIG. 1. (A,B) The 1-tree and 2-tree subgraphs at level $p = 3$, for regularity $d = 3$. (C) The path from outer leaf to root, together with the angle dependencies of each layer. The root variable is shown in black, the other variables are color coded according to their layer: $m = 1$ orange, $m = 2$ green, $m (= p) = 3$ blue.

paper is shown in Fig. 5, where the asymptotic performances of QAOA for both problems are summarized for many different regularities. We conclude in Sec. VI, and provide the full tree calculations in Appendix A.

II. QAOA AND TREE QAOA

In this section, we review the QAOA algorithm, and summarize its asymptotic limit in the number of nodes N for d -regular graphs, which we will refer to as ‘tree QAOA’. QAOA is a variational algorithm that is designed to find low-energy states of a diagonal Hamiltonian H . Our work considers the Ising Hamiltonian on random d -regular graphs $G(V, E) \in \mathbb{G}(N, d)$, with V the vertex set $|V| = N$, and E the edge set $|E| = Nd/2$,

$$H = \frac{1}{\sqrt{d}} \left(\sum_{ij \in E} Z_i Z_j + h \sum_{i \in V} Z_i \right). \quad (1)$$

Here Z_i is the Pauli- Z operator associated with the i th qubit, we use the convention that $Z_i |z\rangle = z_i |z\rangle$ with $z_i \in \{-1, 1\}$ and $\mathbf{z} = (z_1, \dots, z_N)$. To find low-energy states, one optimizes a depth- p parametrized circuit ansatz that has been introduced in Ref. [11]

$$|\gamma, \beta\rangle = \dots e^{-i\beta_p B} e^{-i\gamma_p H} \dots e^{-i\beta_1 B} e^{-i\gamma_1 H} |+\rangle, \quad (2)$$

where $B = \sum_i X_i$ is the mixing operator, with X_i the Pauli- X operators. The initial state is an eigenstate of the mixing operator, and is defined as $|+\rangle = \frac{1}{\sqrt{2^N}} \sum_{\mathbf{z}} |\mathbf{z}\rangle$. Using the Ritz’ variational principle one can find optimal parameters $\beta = (\beta_1, \dots, \beta_p)$ and $\gamma = (\gamma_1, \dots, \gamma_p)$ in a classical outer optimization loop such that the variational energy of the classical cost function, in our case Eq. (1), is minimized

$$\min_{\gamma, \beta} \langle \gamma, \beta | H | \gamma, \beta \rangle. \quad (3)$$

This guarantees that measurement samples \mathbf{z} from the prepared quantum state $|\gamma, \beta\rangle$ on average have low energy $H(\mathbf{z}) = \langle \mathbf{z} | H | \mathbf{z} \rangle$ in a noiseless scenario. Ideally, the optimal solution \mathbf{z}_{opt} , for which $H(\mathbf{z}_{opt}) = \min_{\mathbf{z}} H(\mathbf{z})$, is sampled with non-vanishing probability. The QAOA ansatz is inspired by a trotterization of the quantum annealing protocol and therefore the adiabatic theorem guarantees that this is true for $p \rightarrow \infty$ with unit probability, but this is not practically attainable. It can however be shown that the variational method, where the trotter-step sizes are optimized, always performs better compared to continuous evolution if the total evolution time is finite [58]. Therefore, in this paper we want to investigate which energies (3) can be reached in the limit of large instances $N \rightarrow \infty$ for fixed p .

The energy expectation value (3) consists of a sum of local expectation values, because the summations in Eq. (1) run over the edges and vertices of the problem graph. As the problem graph also determines the two-qubit gates in the QAOA ansatz, it follows that $\langle \gamma, \beta | Z_i | \gamma, \beta \rangle$ only depends on gates acting on qubits that are within distance p in the problem graph from vertex i . All other gates commuting with the measurement operator Z_i , and hence undergo a unitary cancellation. This is true in a similar fashion for $\langle \gamma, \beta | Z_i Z_j | \gamma, \beta \rangle$ with $ij \in E$, i.e. only gates acting on qubits that are within distance p from either i or j contribute. The qubits on which local expectation values depend form a subgraph of the original problem graph. We will refer to the set of gates acting on a subgraph, and determining the expectation value of a local operator, as the Reverse Causal Cone (RCC) of the operator. When uniformly sampling large random regular graphs, the probability of having small loops (e.g. triangles) in the graph

is exponentially suppressed [18]. This fact allows us to assume that all the subgraphs have the same topology when $N \rightarrow \infty$, namely regular trees. Therefore, the energy density measured on the QAOA ansatz state reduces to

$$\lim_{N \rightarrow \infty} \frac{\langle \boldsymbol{\gamma}, \boldsymbol{\beta} | H | \boldsymbol{\gamma}, \boldsymbol{\beta} \rangle}{N} = \frac{\sqrt{d}}{2} \langle \boldsymbol{\gamma}, \boldsymbol{\beta} | Z_1 Z_2 | \boldsymbol{\gamma}, \boldsymbol{\beta} \rangle^{2\text{-tree}} + \frac{h}{\sqrt{d}} \langle \boldsymbol{\gamma}, \boldsymbol{\beta} | Z_1 | \boldsymbol{\gamma}, \boldsymbol{\beta} \rangle^{1\text{-tree}}, \quad (4)$$

where H is given by Eq. (1). The tree subgraphs that are seen by depth $p = 3$ QAOA are illustrated in Fig. 1.

In Appendix A, we provide recursive formulas for the two terms in Eq. (4). These generalize the formulas derived in Ref. [19] by breaking the \mathbb{Z}_2 symmetry of MaxCut, and by including a block symmetry in the iterations. Here, we will only summarize the results of A 1, and refer to the full Appendix A for the derivation and more compact iterations.

The two terms needed to evaluate Eq. (4) are

$$\langle \boldsymbol{\gamma}, \boldsymbol{\beta} | Z_1 Z_2 | \boldsymbol{\gamma}, \boldsymbol{\beta} \rangle^{2\text{-tree}} = \sum_{\mathbf{a}, \mathbf{b}} a_0 b_0 f(\mathbf{a}) f(\mathbf{b}) H_{d-1}^{(p)}(\mathbf{a}) H_{d-1}^{(p)}(\mathbf{b}) \exp\left(i \frac{1}{\sqrt{d}} \boldsymbol{\Gamma} \cdot \mathbf{a} \mathbf{b}\right) \exp\left(i \frac{h}{\sqrt{d}} \boldsymbol{\Gamma} \cdot (\mathbf{a} + \mathbf{b})\right), \quad (5)$$

and

$$\langle \boldsymbol{\gamma}, \boldsymbol{\beta} | Z_1 | \boldsymbol{\gamma}, \boldsymbol{\beta} \rangle^{1\text{-tree}} = \sum_{\mathbf{a}} a_0 f(\mathbf{a}) H_d^{(p)}(\mathbf{a}) \exp\left(i \frac{h}{\sqrt{d}} \boldsymbol{\Gamma} \cdot \mathbf{a}\right). \quad (6)$$

Here,

$$\mathbf{a} = (a_1, \dots, a_p, a_0, a_{-p}, \dots, a_{-1}), \quad a_i \in \{-1, 1\}, \quad (7)$$

are bitstrings of length $2p + 1$, and following the notation of Ref. [19], we also arrange the problem angles in a vector of length $2p + 1$

$$\boldsymbol{\Gamma} = (\gamma_1, \dots, \gamma_p, 0, -\gamma_p, \dots, -\gamma_1), \quad (8)$$

and define the following function containing the mixing angles

$$f(\mathbf{a}) = \frac{1}{2} \langle a_1 | e^{i\beta_1 X} | a_2 \rangle \langle a_2 | e^{i\beta_2 X} | a_3 \rangle \dots \langle a_p | e^{i\beta_p X} | a_0 \rangle \quad (9)$$

$$\langle a_0 | e^{-i\beta_p X} | a_{-p} \rangle \dots \langle a_{-3} | e^{-i\beta_2 X} | a_{-2} \rangle \langle a_{-2} | e^{-i\beta_1 X} | a_{-1} \rangle. \quad (10)$$

The element-wise product between two bitstrings is denoted as $\mathbf{a} \mathbf{b}$, and the inner product between two vectors as $\boldsymbol{\Gamma} \cdot \mathbf{a}$. The notation $\sum_{\mathbf{a}}$ (or $\sum_{\mathbf{a}, \mathbf{b}}$) means summing over one basis set (or two independent basis sets). The recursive iteration is given by

$$H_{d-1}^{(m)}(\mathbf{a}) = \left[\sum_{\mathbf{b}} f(\mathbf{b}) H_{d-1}^{(m-1)}(\mathbf{b}) \exp\left(i \frac{1}{\sqrt{d}} \boldsymbol{\Gamma} \cdot \mathbf{a} \mathbf{b}\right) \exp\left(i \frac{h}{\sqrt{d}} \boldsymbol{\Gamma} \cdot \mathbf{b}\right) \right]^{d-1}, \quad (11)$$

with $m = 1, \dots, p$ and $H_{d-1}^{(0)}(\mathbf{a}) \equiv 1$. Note however, that the subgraph of the local term has only a single root variable. Therefore, it has d equivalent ‘branches’ (and not just $d - 1$), see also Fig. 1. For this reason the final iteration, when $m = p$, needs to be modified in this case to

$$H_d^{(p)}(\mathbf{a}) = \left[\sum_{\mathbf{b}} f(\mathbf{b}) H_{d-1}^{(p-1)}(\mathbf{b}) \exp\left(i \frac{1}{\sqrt{d}} \boldsymbol{\Gamma} \cdot \mathbf{a} \mathbf{b}\right) \exp\left(i \frac{h}{\sqrt{d}} \boldsymbol{\Gamma} \cdot \mathbf{b}\right) \right]^d. \quad (12)$$

In Sec. V, we will discuss our results that follow from minimizing Eq. (4). The time complexity of evaluating the energy density with the above described recursive procedure scales as $O((p + 1)2^{4p+2})$.

III. MAXCUT AND MAXIMUM INDEPENDENT SET AS ISING MODELS

MaxCut refers to the task to find a bipartition of the set of vertices of a given graph into two sets such that the number of edges of the graph connecting nodes between the two sets is maximal. The MIS problem asks for the largest set of vertices for a given graph such that no two vertices within this set are adjacent in the graph. The cost function for both MaxCut and MIS can be described as an Ising Hamiltonian of the form of Eq. (1) which enables us to treat them on a similar footing. We will consider both problems on d -regular graphs with $d \geq 3$. Note that for $d < 3$, the MaxCut and MIS problems are equivalent and trivial.

Regularity d	3	4	5	6	7	8	9	10	20	50	100
c_{ub} (UB cut fraction)	0.92410	0.86824	0.83504	0.80500	0.78509	0.76585	0.75233	0.73877	0.67023	0.60820	0.57665
r_{ub} (UB independence ratio)	0.45400	0.41635	0.38443	0.35799	0.33567	0.31652	0.29987	0.28521	0.19732	0.11079	0.06787

TABLE I. The upper bounds on the optimal cut fraction c_{opt} and independence ratio r_{opt} for d -regular graphs in the asymptotic limit $N \rightarrow \infty$. For the MaxCut problem, these upper bounds have been obtained by solving the variational problem derived in Ref. [47]. For the MIS problem, the upper bounds have been taken directly from Ref. [60], see also Refs. [48, 49].

A. MaxCut

When $h = 0$ the model (1) corresponds to the standard Ising anti-ferromagnet, whose ground state encodes the solution of the MaxCut problem. Indeed, minimizing the energy when $h = 0$, corresponds to maximizing the expected number of cut edges (or anti-ferromagnetic interactions)

$$C = \frac{1}{2} \sum_{ij \in E} (1 - Z_i Z_j). \quad (13)$$

Suppose we have a QAOA ansatz state $|\gamma, \beta\rangle$, obtained by minimizing the energy given by Eq. (1), and we would like to assess the average quality of a candidate solution \mathbf{z} sampled from this quantum state. For the MaxCut problem, finding a performance metric is straightforward, as every basis state \mathbf{z} can be seen as a candidate solution, for which we can calculate the expected ‘cut fraction’ $c \in \{0, 1/|E|, \dots, 1\}$ with $|E| = Nd/2$,

$$c(\mathbf{z}) = \frac{1}{2|E|} \sum_{ij \in E} (1 - \langle \mathbf{z} | Z_i Z_j | \mathbf{z} \rangle). \quad (14)$$

In the limit $N \rightarrow \infty$, the expected cut fraction for the depth- p QAOA ansatz state minimizing the energy (1) is

$$c_p = \lim_{N \rightarrow \infty} \frac{1}{2|E|} \sum_{ij \in E} (1 - \langle \gamma, \beta | Z_i Z_j | \gamma, \beta \rangle) = \frac{1 - \langle \gamma, \beta | Z_1 Z_2 | \gamma, \beta \rangle^{2\text{-tree}}}{2}. \quad (15)$$

In this limit, it has been shown in Ref. [47] that there exist rigorous upper bounds on the optimal cut fraction c_{opt} , $c_{ub} > c_{opt}$, for d -regular graphs (and for sparse Erdős-Rényi graphs), confirming the bounds conjectured in Ref. [59]. These bounds can be obtained from techniques in statistical physics that make use of the interpolation method. In practice, they can be obtained by solving a small variational problem. The solutions of these variational problems are listed in Table I for different graph regularities.

Other upper bounds can be derived from complementary approaches, relating the improvement that is made on top of the average random sampling outcome to the Parisi constant [46]. However, we have found that the first approach yields a tighter (i.e. lower) upper bound on the optimal fraction, at least for small regularities $d < 10$. With the help of the tighter upper bound on the optimal cut fraction c_{ub} , we can compute a tighter (i.e. higher) lower bound α_{MC} on the approximation ratio c_p/c_{opt} , and thus on the performance, of QAOA for MaxCut

$$c_p < \alpha_{MC} = \frac{c_p}{c_{ub}} < \frac{c_p}{c_{opt}} \leq 1. \quad (16)$$

There is a lot of QAOA literature, including the original paper, where the cut fraction c_p itself is considered as a lower bound. While this is naturally correct (a weaker lower bound is still a lower bound), it may suggest the misleading insight that the performance of QAOA is worse for MaxCut on graphs with higher regularity [25]. This is indeed wrong as in the extreme limit of (large) complete graphs, maximal cuts have size $|E|/2$, and such cuts are given on average by random sampling (which is equivalent to $p = 0$ QAOA, or to QAOA with all angles 0). Hence, the MaxCut problem is easy in this limit, and the performance of QAOA should therefore improve.

B. Maximum independent set

The MIS problem is about finding the largest subset of vertices of a given graph such that none of them is sharing an edge. The MIS problem is solved by finding the ground state of

$$H_\lambda^{MIS} = \lambda \sum_{ij \in E} N_i N_j - \sum_{i \in V} N_i \quad (17)$$

with $\lambda > 1$, and the ‘number operator’ $N_i = \frac{Z_i+1}{2}$, therefore $N_i |z_i\rangle \in \{0, 1\}$. We assume that if $N_i |z_i\rangle = 1$, the i -th vertex is part of the chosen set. The second term in Eq. (17) is attempting to maximize the number of vertices in the set, i.e. the number of 1’s in $|z\rangle$, while the first term ensures their independence by adding an energy penalty for having two adjacent vertices in the set. For regular graphs, and in terms of Pauli- Z operators, this Hamiltonian becomes

$$H_{\lambda,d}^{MIS} = \frac{\lambda}{4} \sum_{ij \in E} Z_i Z_j + \frac{\lambda d - 2}{4} \sum_{i \in V} Z_i + \frac{\lambda d N}{8} - \frac{N}{2}. \quad (18)$$

After rescaling $H_{\lambda,d}^{MIS} \rightarrow 4/\lambda H_{\lambda,d}^{MIS}$, we see that this reduces to Eq. (1) with $h = d - 2/\lambda$ up to an irrelevant constant. Hence, the ground state of Eq. (1) corresponds to the solution of the maximum independent set if $h \in]d - 2, d]$. However, the low-lying excited states might not correspond to independent sets. Note that for h ’s outside this interval, even the ground state might not correspond to an independent set. For both reasons, a simple pruning protocol can be devised: if we have a candidate solution $\mathbf{z} \in \{-1, 1\}^{\otimes N}$ with $H_{\lambda=1,d}^{MIS}(\mathbf{z}) = \langle \mathbf{z} | H_{\lambda=1,d}^{MIS} | \mathbf{z} \rangle < 0$, we can prune this bitstring to an independent set of at least size $-H_{\lambda=1,d}^{MIS}(\mathbf{z})$. Indeed, assume that $z_i = z_j = 1$ and that ij is an edge in G . If we remove this edge by flipping one of the variables randomly, the resulting state has at most the same energy $H_{\lambda=1,d}^{MIS}(\mathbf{z})$. States with positive energy $H_{\lambda=1,d}^{MIS}(\mathbf{z}) > 0$ have less vertices chosen than edges existing that connect them. This means the above described pruning procedure might end up in a trivial independent set containing only one vertex. For states with positive energy, we can thus make the worst-case (trivial) assumption that they correspond to a single-node solution by keeping one of the 1’s and flipping all others. Note however, that the single node solution is ‘optimal’ for complete graphs, indeed, for complete graphs we have that the lower bound in the spectrum is $\min_{\mathbf{z}} H_{\lambda=1,d}^{MIS}(\mathbf{z}) = -1$.

Now, we would like to ask the same question as before for MaxCut: suppose we have a QAOA ansatz state $|\gamma, \beta\rangle$, obtained by minimizing the energy given by Eq. (1), what is the average quality of a candidate solution \mathbf{z} sampled from this quantum state? For the MIS problem, not every basis state \mathbf{z} can be seen as a candidate solution, as not every basis state corresponds to an independent set. However, as discussed above, basis states with $H_{\lambda=1,d}^{MIS}(\mathbf{z}) < 0$ are easily prunable, to independent sets of at least size $-H_{\lambda=1,d}^{MIS}(\mathbf{z})$. The independence ratio is given by the number of variables in the independent set divided by the total number of variables. As performance metric for MIS, will thus consider

$$r(\mathbf{z}) = -\frac{H_{\lambda=1,d}^{MIS}(\mathbf{z})}{N} = -\frac{1}{4N} \sum_{ij \in E} \langle \mathbf{z} | Z_i Z_j | \mathbf{z} \rangle - \frac{2-d}{4N} \sum_{i \in V} \langle \mathbf{z} | Z_i | \mathbf{z} \rangle + \frac{4-d}{8}, \quad (19)$$

which is only meaningful when positive. In the asymptotic limit the expected independence ratio of bitstrings sampled from a QAOA state with negative energy $\langle H_{\lambda=1,d}^{MIS} \rangle$ is given by

$$r_p = \lim_{N \rightarrow \infty} \left[-\frac{1}{4N} \sum_{ij \in E} \langle \gamma, \beta | Z_i Z_j | \gamma, \beta \rangle + \frac{2-d}{4N} \sum_{i \in V} \langle \gamma, \beta | Z_i | \gamma, \beta \rangle + \frac{4-d}{8} \right] \quad (20)$$

$$= -\frac{d}{8} \langle \gamma, \beta | Z_i Z_j | \gamma, \beta \rangle^{2\text{-tree}} + \frac{2-d}{4} \langle \gamma, \beta | Z_i | \gamma, \beta \rangle^{1\text{-tree}} + \frac{4-d}{8}. \quad (21)$$

Similarly, as for the cut fraction for the MaxCut problem, the optimal (largest) independence ratio for MIS on d -regular graphs r_{opt} can be upper bounded by a non-constructive method for $N \rightarrow \infty$ [48, 49]. So we can derive a $r_{ub} > r_{opt}$, which can then be used to form a lower bound α_{MIS} on the approximation ratio r_p/r_{opt} achieved by QAOA on this problem in limit of large N

$$r_p < \alpha_{MIS} = \frac{r_p}{r_{ub}} < \frac{r_p}{r_{opt}} \leq 1. \quad (22)$$

The upper bounds r_{ub} are also listed in Table I for different regularities. These have been taken from Ref. [60].

With the above introduced Ising model and performance metrics α_{MC} and α_{MIS} , we will be able to investigate the performance of tree QAOA in solving the MaxCut and MIS problems as a function of the local field. From this section, it may seem intuitive that MIS problem is hard, as the magnitude of the local terms in Eq. (1) exactly balances the magnitude of the interactions. (Recall that the MIS regime is realized when $h \in]d - 2, d]$.) Therefore, the MIS problem is realized exactly in the ‘critical’ h regime of Eq. (1).

It has indeed been shown that the MIS problem exhibits a hardness property known as the ‘overlap gap property’, and that local algorithms cannot find high quality solutions. We will review these topics in the next section.

IV. LOCAL ALGORITHMS AND OVERLAP GAP PROPERTY

Independent sets of more than half the size of the maximum independent set of random regular graphs above a certain degree are either very similar i.e. contain almost the same set of vertices, or very different i.e. contain almost disjoint sets of vertices [50]. In other words, there is a gap in the overlap of large independent sets of graphs, which is why this phenomenon is called the Overlap Gap Property (OGP) of the MIS problem. Other NP-hard optimization problems like MaxCut are not believed to exhibit this phenomenon [43]. There is analytical evidence that this fundamental difference between the combinatorial optimization problems has a profound impact on the performance of local algorithms, classical and quantum alike. Therefore, in this section we will briefly review p -local algorithms, and their performance limitations caused by OGP for the MIS problem.

An intuitive definition of generic p -local algorithms (be it quantum or classical) is given in Ref. [45]. We review this definition tailored to our purposes. We start by defining the p -local environment of a vertex $v_i \in V$ in the problem graph $G(V, E)$ as the subgraph $B_G^p(v_i) \subseteq G(V, E)$ induced by vertex set $\{v_j \in V \mid d_G(v_i, v_j) \leq p\}$. Here the graph distance between two vertices $d_G(v_i, v_j)$ is the number of edges in the shortest path between v_i and v_j .

We consider a probabilistic algorithm \mathcal{A} that generates samples from a distribution $\mathcal{A}_G(z_1, z_2, \dots, z_N)$ of binary variables z_1, \dots, z_N that are associated to each vertex of a specific graph G . We say that \mathcal{A} is a p -local algorithm when it satisfies two criteria:

- (i) $\mathcal{A}_G(z_i) = \sum_{z_1, \dots, z_N \setminus z_i} \mathcal{A}_G(z_1, z_2, \dots, z_N)$ is statistically independent from $\mathcal{A}_G(z_j) = \sum_{z_1, \dots, z_N \setminus z_j} \mathcal{A}_G(z_1, z_2, \dots, z_N)$ when $d(v_i, v_j) > 2p$,
- (ii) $\mathcal{A}_G(z_i) = \mathcal{A}_G(z_j)$ if their p -local environments are isomorphic $B_G^p(v_i) \simeq B_G^p(v_j)$.

In this sense QAOA is a local algorithm because (i) observables with non-overlapping RCCs are not mutually entangled, and (ii) the observables depend solely on the topology of their RCCs.

We now review the definition of the OGP tailored to the MIS problem on regular graphs. Further details can be found in Refs. [37, 50]. We start by considering a multiplicative factor $\mu \in [0, 1]$, that quantifies the distance between a candidate solution and the optimum. For a given graph G , we can thus define the set of μ -good solutions (where we will assume that the bitstring \mathbf{z} corresponds to an independent set of G)

$$\mathcal{S}(\mu, G) = \{\mathbf{z} : r(\mathbf{z}) \geq \mu r_{opt}\}. \quad (23)$$

Now let us consider two random regular graph instances G_0 and G_1 , defined on N vertices, each with their corresponding sets of μ -good solutions. Let us define for every $0 < \theta \leq \mu$, two sets of pairs $(\mathbf{z}_0, \mathbf{z}_1)$ with $\mathbf{z}_i \in \mathcal{S}(\mu, G_i)$, $i = 0, 1$, such that

$$\mathcal{S}^{\text{similar}}(\mu, \theta, G_0, G_1) = \{(\mathbf{z}_0, \mathbf{z}_1) : r(\mathbf{z}_0 \wedge \mathbf{z}_1) \geq \theta r_{opt}\}, \quad (24)$$

and

$$\mathcal{S}^{\text{different}}(\mu, \theta, G_0, G_1) = \{(\mathbf{z}_0, \mathbf{z}_1) : r(\mathbf{z}_0 \wedge \mathbf{z}_1) \leq \theta r_{opt}\}. \quad (25)$$

These sets thus contain pairs of good solutions whose independence ratio of the intersection normalized to the optimal independence ratio, is either equal, or smaller or bigger than θ . Here the intersection of two independent sets means taking the logical AND product between their bitstrings, i.e. element-wise $z_i \wedge z_j = 1$ if and only if $z_i = 1$ and $z_j = 1$.

We now define interpolation graphs G_t between the two random regular graphs G_0 and G_1 . Here $t \in \{0, 1/|E|, \dots, 1\}$ determines the fraction of edges that are selected from G_1 and added to G_t . At the same time a fraction of $(1 - t)$ edges are selected from G_0 and added to G_t . To have similarity between G_t and $G_{t+\Delta}$ with $\Delta = |E|^{-1}$, the previously added (removed) edges from G_1 (G_0) should remain the same, such that G_t and $G_{t+\Delta}$ only differ by two edges in the typical case. For the sake of stating the OGP property of MIS, it does not matter that G_t is not regular at every step in the interpolation. The average regularity of G_t is still d , which is the important fact.

Theorem 1. *The MIS problem on d -regular graphs has OGP when d is large enough. This means that there exist a μ^* such that for every $\mu > \mu^*$ there exists $0 < \theta_1 < \theta_2 < \mu$, such that for N large enough*

$$\mathcal{S}^{\text{similar}}(\mu, \theta_1, G_{t_1}, G_{t_2}) \cap \mathcal{S}^{\text{different}}(\mu, \theta_2, G_{t_1}, G_{t_2}) = \emptyset, \quad \forall 0 \leq t_1, t_2 \leq 1 \quad (26)$$

with high probability (i.e. a probability converging to 1 exponentially fast in N), and

$$\mathcal{S}^{\text{similar}}(\mu, \theta_1, G_0, G_1) = \emptyset \quad (27)$$

with high probability.

Regularity d	3	4	5	6	7	8	9	10	20	50	100
Lower bound on μ^* for MIS	0.9809	0.9705	0.9346	0.9300	0.9255	0.9098	0.9057	0.9021	0.8808	0.8583	0.8427

TABLE II. The lower bounds on the possible onset of OGP for the MIS problem for d -regular graphs in the asymptotic limit $N \rightarrow \infty$. These bounds are the approximation ratios achieved by the linear-time classical algorithm presented in Ref. [60], which is the state-of-the-art classical local polynomial-time algorithm solving this problem.

Hence, the OGP means that for bounded degree random graph instances G_{t_1} and G_{t_2} , pairs of μ -good solutions are either ‘similar’ (they have at least normalized intersection ratios of θ_2), or ‘different’ (they have at most normalized intersection ratios of θ_1) with high probability. Pairs of μ -good solutions that do not satisfy this property are exponentially rare. Additionally, when two graph instances do not share an a priori similarity, like G_0 and G_1 , it is already exponentially rare to have pairs of similar μ -good solutions with normalized intersection ratios larger than θ_1 . This means that somewhere in the interpolation between G_0 and G_1 , there must be a ‘jump’ allowing for pairs of similar solutions.

It is shown in Ref. [50] that the presence of OGP for MIS on regular graphs with large d obstructs local algorithms, like p -local QAOA [37, 38], from finding $(\mu > \frac{1}{2} + \frac{1}{2\sqrt{2}})$ -good solutions with non-vanishing probability. We briefly sketch why. Let us construct a sequence of coupled independent sets for the interpolation graphs G_t , which we call \mathbf{z}_t . This sequence starts from an independent set \mathbf{z}_0 obtained by taking a single sample from running the depth- p QAOA algorithm for G_0 , potentially followed by pruning. QAOA exhibits strong Hamming weight concentration [37]. Therefore, $r(\mathbf{z}_0)$ will not differ much from its average r_p^0 with high probability. Because we know that the next graph G_Δ only differs by at most two edges from G_0 , we can construct an independent set \mathbf{z}_Δ that is similar to \mathbf{z}_0 . Indeed, as G_Δ only differs by at most two edges from G_0 , there exist QAOA samples for G_Δ that will only be different in at most $4 \max_i |B_G^p(v_i)|$ bits from \mathbf{z}_0 . We take \mathbf{z}_Δ to be one of those. Notice that for fixed p and large N , the subgraph sizes are vanishing compared to N , so that is why \mathbf{z}_0 and \mathbf{z}_Δ are considered similar. Like this we can construct the sequence of similar solutions \mathbf{z}_t .

We now assume that depth- p QAOA can create large independent sets of G_t

$$r_p^t > \mu r_{opt}. \quad (28)$$

Notice that concentration over graph instances [18] implies that assumption (28) must be valid $\forall t$. However this assumption is in direct violation with the OGP of MIS **Theorem 1**, because it would then be possible with high probability to have similar large independent sets, for which $\mathbf{z}_0 \wedge \mathbf{z}_t$ is large, without having a sudden jump to different large independent sets, for which $\mathbf{z}_0 \wedge \mathbf{z}_{t+\Delta}$ is small, for a certain t . Therefore, we conclude that the expected independence ratio obtained from QAOA is suboptimal for large enough N and d

$$r_p \leq \mu r_{opt}. \quad (29)$$

It is shown in Ref. [61] that asymptotically $\mu^* \gtrsim 1/2$, for $d \rightarrow \infty$. Hence, there is a performance gap that can be as large as $1/2$ between the output of local algorithms and optimality. (Famously, this is also true for Erdős-Rényi graphs that are both sparse and dense [62, 63].) Indeed, it is shown in Ref. [64] that the optimal (i.e. maximum) independence ratio asymptotically converges to $2 \log(d)/d$, for $d \rightarrow \infty$. However, it is shown in Ref. [61] that the largest independence ratios that can be obtained by local algorithms are asymptotically $\log(d)/d$, when $d \rightarrow \infty$.

These findings refuted the hope [65] that local algorithms may be able to find maximum independent sets in random regular graphs. However, the statements are only proven for ‘sufficiently large’ d , which leaves open the question if OGP holds for the smallest d , and if it holds, what would be the value of μ^* . From Ref. [60], some lower bounds for the possible onset of OGP can however be deduced, see Table II. Hence, the regularities considered in this paper seem still rather far from the asymptotic d regime. This also implies that even if there is OGP existing for the smallest regularity graphs, the regime in which it exists is small. Indeed, for instance for $d = 3$, Table II means that there exists a local algorithm that can create independent sets with ratios of at least $0.9809 r_{opt}$. Hence if the MIS problem for $d = 3$ would have an OGP, μ^* must be bigger than this value. In other words, local algorithms fail the earliest in creating independent sets with ratios larger $0.9809 r_{opt}$ if the MIS for $d = 3$ problem would have an OGP.

In general, a proven presence of OGP for a problem class, yields a limitation on the performance of *all* local algorithms [42, 45]. On the other hand, it is a standing conjecture that the MaxCut (and Sherrington-Kirkpatrick) problems do not have OGP [43–45], and that there is thus no such performance gap set by a certain μ^* for local algorithms. Indeed, under the assumption that these problems have no OGP, approximate message-passing algorithms have been devised that with high probability do not see such a gap [34, 66]. In Ref. [34] in particular, such an algorithm

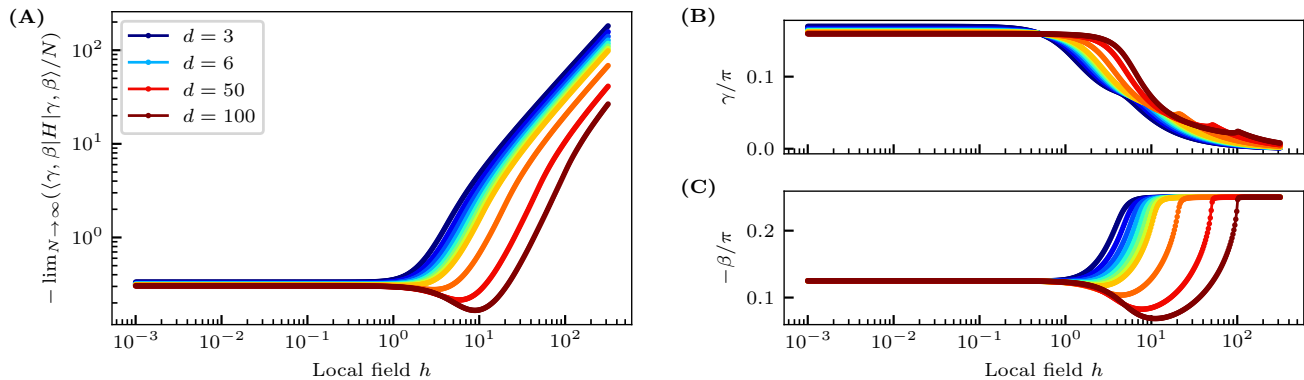


FIG. 2. **(A) The asymptotic energy densities** achieved by $p = 1$ QAOA as a function of the local field [see Eq. (4)]. The colors indicate the different graph regularities listed in Table I, only a selection is shown in the legend. **(B,C) The respective QAOA angles to obtain these energy densities.**

for the MaxCut problem is constructed that finds solutions that are $(1 - \epsilon)$ close to optimality with high probability. It relies however on the condition that $d > O(1/\epsilon)$. Hence ϵ can not be made arbitrarily small yet.

The conjecture of ‘no OGP’ for MaxCut suggests that there are no bounds on the expected performance of tree QAOA in the asymptotic limit when p is increased. On the other hand, for MIS the regime with OGP can certainly not be reached with p -local QAOA when the RCCs do not span the whole system [37, 38]. The tree QAOA, which is the subject of this paper, however considers the asymptotic limit $N \rightarrow \infty$ and fixed p . In that case, it is also expected that even when increasing p indefinitely, the performance of tree QAOA is bounded away from optimality [67].

In the next section, we will evaluate the performance of tree QAOA explicitly for both problems.

V. TREE QAOA RESULTS

In this section, we first present the results from numerically evaluating the recursive tree QAOA formulas [see Eqs. (6),(5),(11) and (12)] in order to minimize the Ising energy density Eq. (4). These formulas were summarized in their simplest form in Sec. II, and are derived (and made faster, by prefactors) in Appendix A. Second, we recycle the angles obtained from the tree QAOA to solve finite-size instances. In this way, we see that for regularity $d = 3, 4$, we outperform the GW algorithm on average for MaxCut. For MIS, we outperform a minimal greedy algorithm for $d = 3$.

A. Performance of tree QAOA in the asymptotic limit

As a first step, we will optimize the QAOA angles such that the energy density Eq. (4) is minimized as a function of the local field. Secondly, we will evaluate the performance metrics presented in Sec. III on the resulting ansatz state for both problems. Here, the operator in the phase separator of the QAOA ansatz is the same as the objective function that is minimized (i.e. Eq. (1)), but is not necessarily equivalent to the performance metric. Indeed for MaxCut they are only directly related when $h = 0$, and for MIS when $h = d - 2$. Later we will however restrict to these cases. We first investigate the (fixed) performance metrics for both problems as a function of the local field because in that way we can view the performance for different regularities and fields in a unified way. Like that, we can also investigate the QAOA performance of MaxCut in the h -regime for MIS, and conversely. Such analysis leads to interesting observations like that QAOA performs more or less equivalent for both problems, when both d and p are small.

1. Changing the local field

In Fig. 2(A), we show the resulting energy density Eq. (4) as a function of the local field for $p = 1$. The corresponding QAOA angles to obtain these energy densities are shown in Fig. 2(B,C). The behavior of these is quite intuitive: for small $h < 1$ there is an anti-ferromagnetic regime (constant non-trivial γ), for $1 < h < d$ a transition regime (changing

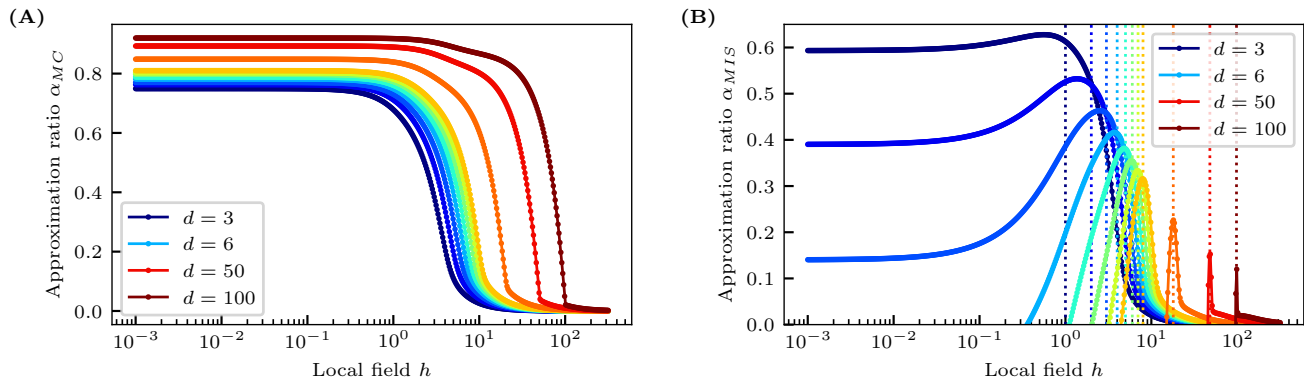


FIG. 3. **The approximation ratios for (A) MaxCut and (B) MIS** obtained by $p = 1$ QAOA optimized as a function of the local field for $N \rightarrow \infty$. The colors indicate the different graph regularities listed in Table I, only a selection is shown in the legend. The dotted vertical lines indicate local fields $h = d - 2$. The QAOA angles are chosen such that the energy density given by Eq. (4) is minimized [see Fig. 2]. The approximation ratios α_{MC} and α_{MIS} as discussed in Sec. III, are evaluated on the resulting QAOA state.

non-trivial angles), and for $d < h$ a trivial regime where all spins simply anti-align with the local field (realized exactly by the $\exp(i\pi/4 \sum_i X_i)$ rotation, and vanishing γ).

In Fig. 3, we show the corresponding asymptotically achieved approximation ratios for the two problems as a function of the local field. These approximation ratios are defined in Sec. III, and take into account the state-of-the-art asymptotic upper bounds listed in Table I. Here, we recall that the zero on the scale means cutting no edges for MaxCut, or finding a vanishing independence ratio with N for MIS. The behaviour of these approximation ratios is interesting. First, we can observe the manifestly different problem hardness when d grows larger in the performance of QAOA for both problems. On the one hand, MaxCut in the large d limit becomes easier. Indeed, when approaching complete graphs, cutting half of the edges (or random sampling), becomes optimal. However, on the other hand MIS is highly non trivial as it has a proven OGP when d grows large [50]. This is reflected by the fact that the maximal approximation ratios achieved by QAOA grow larger with d for MaxCut, while they clearly shrink for MIS. Interestingly, for MIS on 3-regular graphs, the approximation ratio achieved by $p = 1$ QAOA is surprisingly constant when $h < 3$ [see Fig. 3(B)]. This implies that solutions for MIS on 3-regular graphs with independence ratios that are $\sim 60\%$ of the optimum can be equally well sampled from a QAOA circuit with angles optimized for the MaxCut problem. This constant behavior is specific to low regularities and relatively low approximation ratios, and is expected to vanish with increasing d (or p).

There is a sharp transition in the achieved approximation ratios for both problems when $h/d > 1$. This transition is due to the fact that the trivial regime is entered where all spins simply anti-align with h , leading to a diamagnetic state that represents an empty set and that cuts no edges. As QAOA captures this behavior more accurately with increasing p , this transition gets also sharper with increasing p . This can be seen from Fig. 4, where $d = 6$ is fixed, and p increased.

For the MIS case, the performance disappears when h falls below some threshold value if d is large enough. From Figs. 3(B) and 4(B), it can be seen that this happens when $d = 6$ for $p = 1$. Increasing h towards $d - 2$ resolves this behavior, but notice that also increasing p helps to resolve this behavior. For $d = 6$, taking $p = 2$ seems already sufficient [see Fig. 4(B)].

As expected from the problem definition in Sec. III, the MIS approximation ratio reaches a peak when h is around d , corresponding to a positive independence constraint. Interestingly, however, for small p the maximal performance seems to be reached when $h \lesssim d - 2$ corresponding to an independence constraint $\lambda \lesssim 1$. This indicates that the QAOA is broadly centred around low-energy states for $p = 1$. Therefore, it is not a requirement that h is chosen in such a way that the ground state of Eq. (1) corresponds to the maximum independent set. However, when p is increased and when therefore the energy distribution of QAOA shifts towards lower energies, the peak in optimal performance shifts towards a field that corresponds to an independence constraint $\lambda > 1$. This behavior can be seen in Fig. 4(B), where the boundaries of the region with independence constraint $\lambda > 1$ are indicated by the two dashed lines.

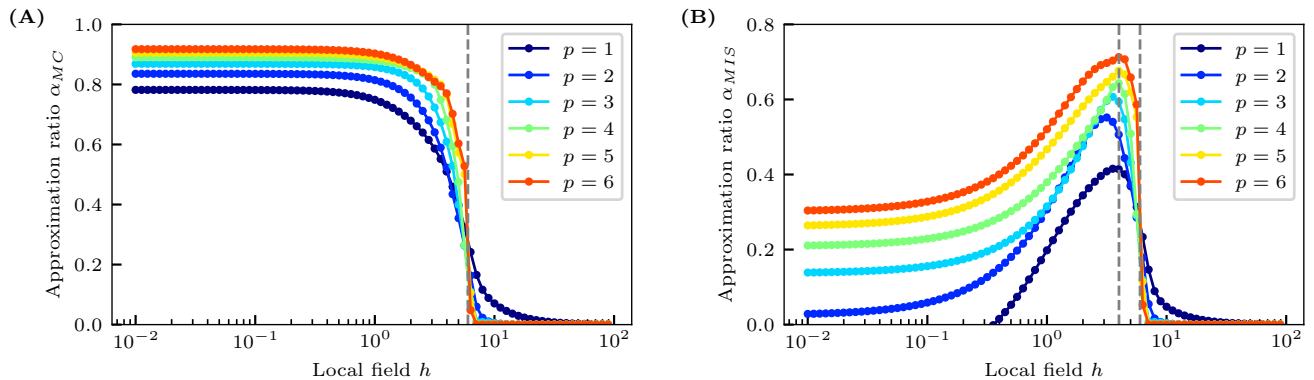


FIG. 4. **The approximation ratios obtained by QAOA for (A) MaxCut, and (B) MIS on 6-regular graphs for various p in the limit $N \rightarrow \infty$.** The QAOA ansatz is optimized to minimize the energy given by Eq. (1). Therefore, there is a sharp transition in solution quality at $h = d$ for both problems. The ground state of Eq. (1) corresponds to the solution of MaxCut when $h \ll d$, and to the solution of MIS when $h \in]d - 2, d]$. In these indicated regions the approximation ratio must therefore increase with p .

2. Fixing the local field

Now, we fix the local field to $h = 0$ for MaxCut and to $h = d - 2$ for MIS (corresponding to $\lambda = 1$), and investigate the performance of tree QAOA with increasing p for different graph regularities. For MaxCut the performance of tree QAOA has been investigated in the literature before [19, 21, 25, 26], it even has been considered for $p = 1$ in the original QAOA paper [11]. However, our current work extends these analyses by: (i) further improving the achieved approximation ratios by employing the upper bounds as discussed in Sec. III, and (ii) extending the analysis to regularities larger than $d = 3$. To make the first point explicit, it is stated in the original QAOA paper that on 3 regular graphs, QAOA is guaranteed to find approximation ratios of at least ~ 0.69 (also for $N \rightarrow \infty$). By incorporating the upper bound on the cut fraction of 3-regular graphs, we realize the approximation ratio is actually at least ~ 0.75 for $N \rightarrow \infty$, see Fig. 5(A). Here, we compare the improved approximation ratios obtained by QAOA, with the guaranteed approximation ratio of the Goemans-Williamson (GW) algorithm [30]. The GW algorithm is guaranteed to find a solution to the MaxCut problem with an approximation ratio of at least $\alpha_{GW} = \min_{x \in [0,1]} 2 \arccos(x) / (\pi(1-x)) = 0.87\dots$ for any instance. Indeed, denoting the cut fraction of a GW solution as c_{GW} , we have that

$$\alpha_{GW} c_{opt} \leq \alpha_{GW} c_{sdp} \leq c_{GW}, \quad (30)$$

where c_{opt} is the cut fraction corresponding to the maximum cut, and c_{sdp} the ‘cut fraction’ corresponding to the solution of the semi-definite program following the relaxation of the binary variables to unit vectors on the N -dimensional sphere. Thus, the knowledge of a tighter upper bound on c_{opt} does not alter the performance guarantee α_{GW} of the GW algorithm. So the approximation ratios introduced in Sec. III compare directly to α_{GW} , and already pass α_{GW} at $p = 4$ for the lowest regularities. However, we expect that the practically achieved GW approximation ratios will improve with increasing d . In particular, they will never fall below the ones of random sampling $(2c_{ub})^{-1}$ shown by the red line in Fig. 5(A). On the other hand, for small d , we already pass α_{GW} at $p = 4$ which leaves open the possibility that shallower circuits than previously assumed could already provide a performance and runtime advantage over the GW algorithm.

For MIS it is up to our knowledge the first time that the tree angles have been calculated, and used to estimate the asymptotic performance. We show the obtained approximation ratios in Fig. 5(B). We compare to the performance guarantee of the minimal greedy algorithm. The minimal greedy algorithm makes locally minimal random choices. It consists out of the following steps: (i) Randomly select a vertex from G that has the lowest regularity. (ii) Add this vertex to the independent set, and delete all its neighbors from G . (iii) Repeat (i) and (ii) until the the graph G is empty (i.e. has no edges left). (iv) Add possible remaining vertices to the independent set. This algorithm is guaranteed to find independent sets with approximation ratios $3/(d+2)$ [69]. We also compare to the best known classical linear-time algorithm of Ref. [60], see dashed grey line. (These approximation ratios are the values that we considered as a lower bound for μ^* in Table II.) As can be seen, there is an increasing gap with d between the approximation reached by QAOA and this algorithm. Therefore, it seems that the performance of tree QAOA for MIS is vanishing upon increasing d . This observation can be made explicit for $p = 1$ [see Appendix A 4], and is expected

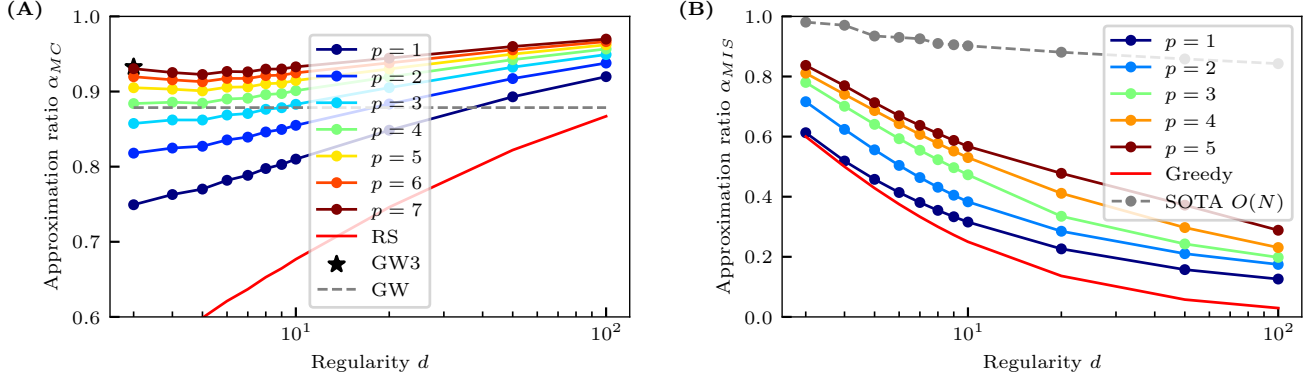


FIG. 5. **The approximation ratios for (A) MaxCut and (B) MIS** obtained by depth- p QAOA for $N \rightarrow \infty$. For MaxCut, we compare with the GW guarantee and Random Sampling (RS). For 3-regular graphs there is a specialized version of the GW algorithm, discussed in Ref. [68], achieving an approximation ratio of 0.9326 which is indicated by the star. For MIS, we compare to the performance guarantee of a minimal greedy search [69], and the state-of-the-art linear-time prioritized search algorithm of Ref. [60].

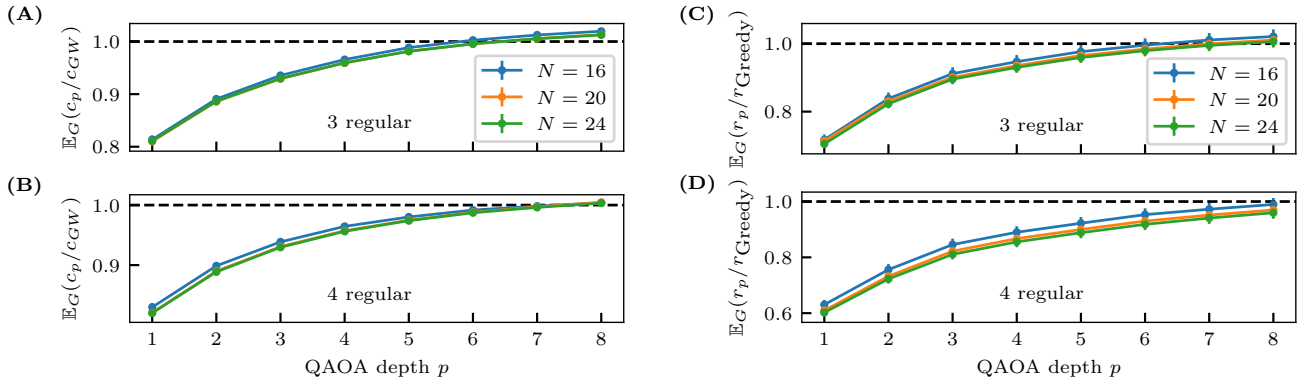


FIG. 6. **Performance comparison between QAOA with predetermined tree angles and classical algorithms** on small instances of 3 and 4 regular graphs. The tree angles have been determined by the techniques outlined in Appendix A. (A,B) **MaxCut QAOA compared to GW**. The comparison is made on an instance-by-instance basis: we compare the expectation value of the number of cut edges measured on the QAOA state with the average number of cut edges based on 100 GW runs. (C,D) **MIS QAOA compared to minimal greedy**. We sampled 200 random graph instances, and the error bars show $3\bar{\sigma}$ with $\bar{\sigma}$ the standard error of the mean. The QAOA angles used for these simulations are included in Appendix B.

to be true as well when $p > 1$. In practice, we are however mostly interested in solving the problems for small and fixed d . Then, the optimal parameters obtained from the tree QAOA could also be used for small problems, of the size of currently available QPU's. Illustrating that this approach achieves good performances is the topic of the next section.

B. Tree QAOA angles applied to finite-size problems

The goal of this section is to compare how well QAOA with the tree angles obtained in the previous section performs for finite-size instances. In the previous section [see Fig. 5], we compared the expected QAOA outcomes with the performance guarantees of classical algorithms (GW for MaxCut and minimal greedy for MIS). However, it may be that in practice the classical algorithms perform significantly better than their lower bound. At the same time, the tree angles are only guaranteed to be optimal in the asymptotic limit (although for MaxCut, it has been observed before that such angles work well away from the asymptotic limit [21, 26].)

To shine a clearer light on these issues, our goal is to make an explicit comparison for both MaxCut and MIS to the classical algorithms. The protocol we use is the following: (i) Use a set of tree angles determined as before (by making

use of the formulas in Appendix A) to create a QAOA ansatz state for the sampled finite-size problem instances $G(N, d)$. Hence, we do not apply a procedure to fine tune the QAOA angles, but use the same set of fixed angles for all. (ii) Measure the performance metrics, i.e. the expectation values of Sec. III, on this QAOA ansatz state. (iii) Run a classical probabilistic algorithm on the same instance a certain number of times, and take the average. (iv) Compare the outcomes of both algorithms.

For MaxCut, we set $h = 0$ in Eq. (1) and compare the fixed angle QAOA to the GW algorithm [30]. We measure the expected number of cut edges in the prepared QAOA state for every instance. For each instance, we then run the GW algorithm 100 times, and take the average. We observed that in practice, in our setup, the GW performs on average significantly better than its worst-case guarantee α_{GW} . This also explains why we only observe an improvement for $p = 8$ for 3 and 4 regular graphs, see Fig. 6(A,B). This is in contrast to the asymptotic limit, where tree QAOA already outperforms the *lower bound* at $p = 4$ [see Fig. 5]. Although the approximation ratios shown in Fig. 5 clearly increase when growing d , we observe for higher p a non-monotonic regime when d is small. This possibly explains the slightly worse performance for $d = 4$ compared to $d = 3$ in Fig. 6(A,B).

For MIS, we set $h = d - 2$ in Eq. (1) and compare to the minimal greedy algorithm. Such greedy algorithms are widely used algorithms, but their performance is not optimal, even among local algorithms. Indeed, from Fig. 5(B), it is clear that we are far from outperforming the state-of-the-art classical local linear-time algorithm that solves the MIS problem in regular graphs [60]. We choose to compare to the greedy algorithm because it represents a lower bound on the performance of classical polynomial-time algorithms. Furthermore, it has a straightforward implementation, and a performance guarantee. Thus, we can still understand how the observation shown in Fig. 5(B) of outperforming its lower bound for any $p \geq 1$ shifts when comparing average outcomes for finite-size instances. This comparison is shown in Fig. 6(C,D) for 3 and 4 regular graphs. We see that the tree QAOA is outperforming the minimal greedy for $p = 8$ in case $d = 3$, however this is not anymore the case for $d = 4$. This confirms that also the greedy algorithm performs significantly better on average than its guarantee. Additionally, it also confirms that the observation of Fig. 5(B), that MIS becomes harder for QAOA when d is larger, is also valid for finite sizes when compared to greedy.

The tree angles we have used for the simulations in this section are included in Appendix B.

VI. CONCLUSION

In this paper, we have investigated the performance of tree QAOA for the MaxCut and MIS problems by unifying them as Ising models. For the MIS problem in particular, this was the first time such an analysis was explicitly performed, up to our knowledge. Our main results are the approximation ratios achieved by QAOA in the limit $N \rightarrow \infty$ shown in Fig. 5 for many different graph regularities. We obtained those by improving on the evaluation of the recursive formulas that describe the contraction sequence from outer ‘leaf’ to ‘root’ in the trees that form the typical (distance- p) subgraphs of large random regular graphs [see Appendix A for the full calculation]. We combine these QAOA results with state-of-the-art upper bounds on optimality for the respective problems [see Tab. I]. For MaxCut we obtained those bounds by using the variational method described in Ref. [47]. This resulted in better approximation ratios than the Goemans-Williamson guarantee already at QAOA depth $p = 4$. For MIS, upper bounds on the independence ratio have been established in Ref. [48, 49]. For this problem, QAOA at any depth $p \geq 1$ outperforms the lower bound of the greedy algorithm. However, QAOA is far from outperforming the best classical local polynomial-time algorithm for this problem [60]. For higher regularity, the performance of QAOA with fixed p is bounded away from optimality for the MIS problem due to the presence of OGP [37, 38]. The increased hardness of the MIS problem with increasing d is clearly manifested by the decrease of approximation ratios achieved by tree QAOA [see Fig. 5]. This behavior is opposite for MaxCut, in this case QAOA achieves better approximation ratios with increasing d , and is believed not to exhibit an OGP.

In addition, we also showed that QAOA has a promising performance when the tree angles are taken as ‘fixed angles’ for small problems. For MaxCut, QAOA with fixed angles outperforms the GW algorithm at $p = 8$ for $d = 3, 4$ when comparing to explicit GW runs. Such an analysis seems to also hold for the MIS problem when comparing to minimal greedy at low regularity. Indeed, in case of $d = 3$, we have outperformed the minimal greedy algorithm with QAOA at depth $p = 8$ when comparing to explicit greedy runs for small instances. The above-mentioned values of $p \geq 4$ (for MaxCut) and $p \geq 1$ (for MIS) of when QAOA outperforms the respective classical algorithms in the limit $N \rightarrow \infty$ compare only to their lower bound. This in combination with finite-size effects is the reason why we needed higher depths of $p \approx 8$ to outperform the classical algorithms for small N .

In order to boost performance, we believe that hybrid quantum-classical approaches are promising [51–57]. Such approaches combine quantum input, for instance $\langle Z_i \rangle$ and $\langle Z_i Z_j \rangle$ measurements on a quantum state, e.g. a QAOA state, with a classical algorithm to produce good solutions. In particular, when the quantum circuit is non-local such approaches may be very effective, although less reachable on the near term. It is however our hope that the tree QAOA angles will serve useful for these approaches, especially for the MIS problem. In that way, expensive and hard

parameter optimization loops can be avoided [70–72], and expected ‘fixed-angle’ performances can be derived.

VII. ACKNOWLEDGEMENTS

We thank Thomas Cope and Jalil Khatibi Moqadam for useful discussions. We also thank Thomas Cope for careful reading and comments on the manuscript. This project is supported by the Federal Ministry for Economic Affairs and Climate Action on the basis of a decision by the German Bundestag through the project Quantum-enabling Services and Tools for Industrial Applications (QuaST). QuaST aims to facilitate the access to quantum-based solutions for optimization problems.

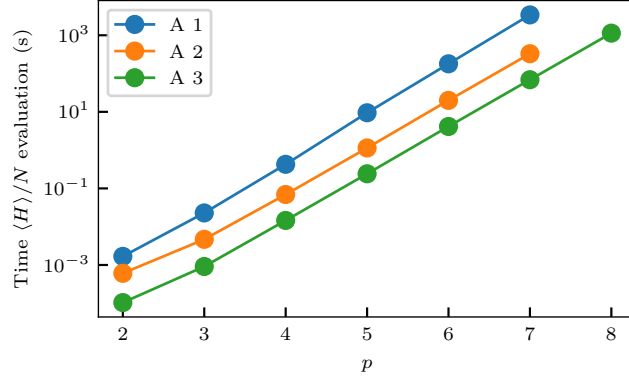


FIG. 7. The computational time, on a single core of a standard laptop, to evaluate Eq. (4) at fixed QAOA angles using the formulas derived respectively in Sections A 1, A 2 and A 3. The speedups obtained are prefactors, the overall scaling remains $O(2^{4p})$.

Appendix A: Calculation of the QAOA expectation values on trees

Our goal is to derive expressions that analytically describe the expectation values in Eq. (4) as recursive formulas. These ideas have been pioneered in Refs. [19, 35]. The latter contains very elegant expressions for the QAOA correlators in the $d \rightarrow \infty$ limit. However the finite- d case received less attention in their work. The calculations as presented in this work are in close correspondence to the ones presented in Ref. [19] with the following differences, each discussed in a different section: (i) We have a local field in our model, and thus have no \mathbb{Z}_2 symmetry, resulting in less symmetric expressions, see A 1. (ii) We grow the basis size at every recursion step, resulting in a faster recursion, see A 2. (iii) We associate a symmetry label t with every basis state, characterizing how ‘time-reversal’ symmetric it is, see A 3. The corresponding computational times of evaluating Eq. (4) according to the three different procedures are shown in Fig. 7. In Fig. 8, we sketch symbolically how these speedups are achieved.

1. A recursive iteration with local field

In this section, our goal is to write down similar expressions as in Ref. [19] with a local field added. For this, we work out

$$\langle \gamma, \beta | Z_1 Z_2 | \gamma, \beta \rangle^{2\text{-tree}} = \langle + | e^{i\gamma_1 H} e^{i\beta_1 B} \dots e^{i\gamma_p H} e^{i\beta_p B} Z_1 Z_2 e^{-i\beta_p B} e^{-i\gamma_p H} \dots e^{-i\beta_1 B} e^{-i\gamma_1 H} | + \rangle, \quad (\text{A1})$$

and

$$\langle \gamma, \beta | Z_1 | \gamma, \beta \rangle^{1\text{-tree}} = \langle + | e^{i\gamma_1 H} e^{i\beta_1 B} \dots e^{i\gamma_p H} e^{i\beta_p B} Z_1 e^{-i\beta_p B} e^{-i\gamma_p H} \dots e^{-i\beta_1 B} e^{-i\gamma_1 H} | + \rangle. \quad (\text{A2})$$

Here H is given by Eq. (1) and is restricted to the trees shown in Fig. 1. These trees are fully characterized by the regularity d and the QAOA depth p . As a first step, we can insert $2p + 1$ resolutions of identity, labelled by $[1], [2], \dots, [p], [0], [-p], \dots, [-2], [-1]$. The basis vectors $\tilde{\mathbf{z}}^{[m]}$ have a dimension that is equal to the number of variables in the tree, i.e.

$$\tilde{\mathbf{z}}^{[m]} = (z_1^{[m]}, z_2^{[m]}, \dots, z_{N_{\text{tree}}}^{[m]}), \quad z_i^{[m]} \in \{-1, 1\} \text{ with } i = 1, \dots, N_{\text{tree}} \quad (\text{A3})$$

For the two different tree variants, this numbers are

$$N_{2\text{-tree}} = 2 \frac{(d-1)^{p+1} - 1}{d-2}, \quad N_{1\text{-tree}} = 1 + d \frac{(d-1)^p - 1}{d-2} \quad (\text{A4})$$

With this, we have that

$$\langle \gamma, \beta | Z_1 Z_2 | \gamma, \beta \rangle^{2\text{-tree}} = \frac{1}{2^{N_{2\text{-tree}}}} \sum_{\{\tilde{\mathbf{z}}\}} \left[z_1^{[0]} z_2^{[0]} \left(\langle \tilde{\mathbf{z}}^{[1]} | e^{i\beta_1 B} | \tilde{\mathbf{z}}^{[2]} \rangle \langle \tilde{\mathbf{z}}^{[2]} | e^{i\beta_2 B} | \tilde{\mathbf{z}}^{[3]} \rangle \dots \langle \tilde{\mathbf{z}}^{[p]} | e^{i\beta_p B} | \tilde{\mathbf{z}}^{[0]} \rangle \right. \right. \quad (\text{A5})$$

$$\left. \langle \tilde{\mathbf{z}}^{[0]} | e^{-i\beta_p B} | \tilde{\mathbf{z}}^{[-p]} \rangle \dots \langle \tilde{\mathbf{z}}^{[-3]} | e^{-i\beta_2 B} | \tilde{\mathbf{z}}^{[-2]} \rangle \langle \tilde{\mathbf{z}}^{[-2]} | e^{-i\beta_1 B} | \tilde{\mathbf{z}}^{[-1]} \rangle \right) \quad (\text{A6})$$

$$\exp\left(i\gamma_1 H(\tilde{\mathbf{z}}^{[1]}) + \dots + i\gamma_p H(\tilde{\mathbf{z}}^{[p]}) - i\gamma_1 H(\tilde{\mathbf{z}}^{[-1]}) - \dots - i\gamma_p H(\tilde{\mathbf{z}}^{[-p]})\right). \quad (\text{A7})$$

Here $\sum_{\{\tilde{\mathbf{z}}\}}$ means summing over all $2p+1$ basis sets, that each have dimension $2^{N_{2\text{-tree}}}$, $H(\tilde{\mathbf{z}}^{[m]})$ represents the energy of the bitstring. Using the same notation as in Ref. [19], we now define the vectors of length $(2p+1)$

$$\mathbf{\Gamma} = (\gamma_1, \dots, \gamma_p, 0, -\gamma_p, \dots, -\gamma_1), \quad (\text{A8})$$

and

$$\mathbf{z}_k = (z_k^{[1]}, \dots, z_k^{[p]}, z_k^{[0]}, z_k^{[-p]}, \dots, z_k^{[-1]}), \quad z_k^{[m]} \in \{-1, 1\} \text{ with } k \in V_{\text{tree}}. \quad (\text{A9})$$

We also separate the β -dependence in the function

$$f(\mathbf{z}_k) = \frac{1}{2} \langle z_k^{[1]} | e^{i\beta_1 X_k} | z_k^{[2]} \rangle \langle z_k^{[2]} | e^{i\beta_2 X_k} | z_k^{[3]} \rangle \dots \langle z_k^{[p]} | e^{i\beta_p X_k} | z_k^{[0]} \rangle \quad (\text{A10})$$

$$\langle z_k^{[0]} | e^{-i\beta_p X_k} | z_k^{[-p]} \rangle \dots \langle z_k^{[-3]} | e^{-i\beta_2 X_k} | z_k^{[-2]} \rangle \langle z_k^{[-2]} | e^{-i\beta_1 X_k} | z_k^{[-1]} \rangle. \quad (\text{A11})$$

The expectation values are

$$\langle z_k^{[m]} | e^{i\beta_i X_k} | z_k^{[n]} \rangle = \begin{cases} \cos(\beta_i), & \text{if } z_k^{[m]} = z_k^{[n]} \\ i \sin(\beta_i), & \text{otherwise,} \end{cases} \quad (\text{A12})$$

and normalization implies that $\sum_{\mathbf{z}_k} f(\mathbf{z}_k) = 1$. With these notations, we have that

$$\langle \gamma, \beta | Z_1 Z_2 | \gamma, \beta \rangle^{2\text{-tree}} = \sum_{\{\mathbf{z}\}} \left[z_1^{[0]} z_2^{[0]} \left(\prod_{k \in V_{2\text{-tree}}} f(\mathbf{z}_k) \right) \exp\left(i \frac{1}{\sqrt{d}} \sum_{kl \in E_{2\text{-tree}}} \mathbf{\Gamma} \cdot \mathbf{z}_k \mathbf{z}_l\right) \exp\left(i \frac{h}{\sqrt{d}} \sum_{k \in V_{2\text{-tree}}} \mathbf{\Gamma} \cdot \mathbf{z}_k\right) \right]. \quad (\text{A13})$$

Here $\sum_{\{\mathbf{z}\}}$ should now be read as summing over all $N_{2\text{-tree}}$ basis sets, that each have dimension 2^{2p+1} , $\mathbf{z}_k \mathbf{z}_l = (z_k^{[1]} z_l^{[1]}, z_k^{[2]} z_l^{[2]}, \dots)$ is the elementwise product of the two bitstrings, and $\mathbf{\Gamma} \cdot \mathbf{z}_k$ the standard inner product between vectors. Up to now we have not exploited the tree structure yet. This structure is however quite easy to impose: there are only connections between ‘generations’, therefore it is natural to rearrange the summation such that we start summing from the outer leaves. Let us label an outer ‘leaf’ by the position index u , and call the ‘parent’ of that leaf $p(u)$. The dependency in Eq. (A13) on this outer leaf can be separated as

$$\sum_{\mathbf{z}_u} f(\mathbf{z}_u) \exp\left(i \frac{1}{\sqrt{d}} \mathbf{\Gamma} \cdot \mathbf{z}_u \mathbf{z}_{p(u)}\right) \exp\left(i \frac{h}{\sqrt{d}} \mathbf{\Gamma} \cdot \mathbf{z}_u\right). \quad (\text{A14})$$

As there are $d-1$ (independent) incoming leaves in the parent node $p(u)$, we can define

$$H_{d-1}^{(1)}(\mathbf{z}_{p(u)}) = \left[\sum_{\mathbf{z}_u} f(\mathbf{z}_u) \exp\left(i \frac{1}{\sqrt{d}} \mathbf{\Gamma} \cdot \mathbf{z}_u \mathbf{z}_{p(u)}\right) \exp\left(i \frac{h}{\sqrt{d}} \mathbf{\Gamma} \cdot \mathbf{z}_u\right) \right]^{d-1}. \quad (\text{A15})$$

Then, we can move inwards and separate the dependencies of $\mathbf{z}_{p(u)}$, and so on. This will lead to the iterations

$$H_{d-1}^{(m)}(\mathbf{a}) = \left[\sum_{\mathbf{b}} f(\mathbf{b}) H_{d-1}^{(m-1)}(\mathbf{b}) \exp\left(i \frac{1}{\sqrt{d}} \mathbf{\Gamma} \cdot \mathbf{a} \mathbf{b}\right) \exp\left(i \frac{h}{\sqrt{d}} \mathbf{\Gamma} \cdot \mathbf{b}\right) \right]^{d-1}, \quad (\text{A16})$$

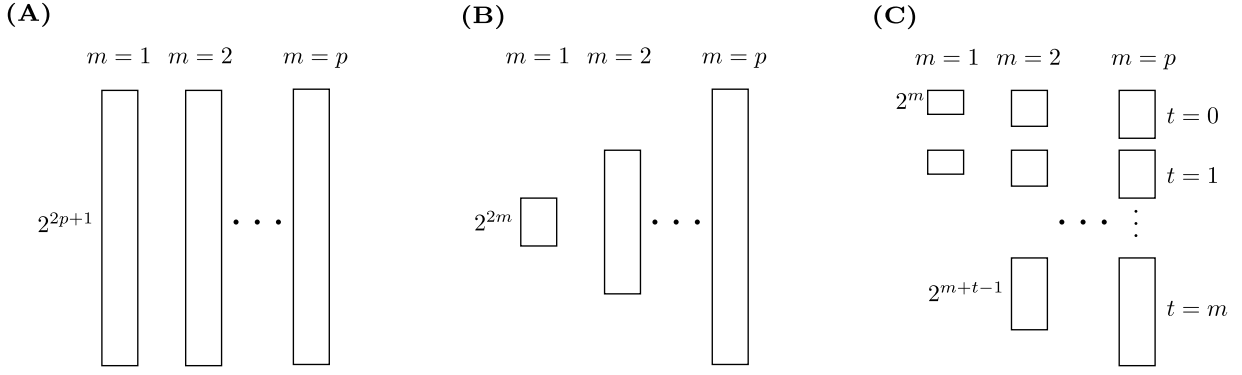


FIG. 8. Structure of the basis at every iteration step $m \in \{1, 2, \dots, p\}$. (A) In the most naive way the basis has the same size 2^{2p+1} at each step. (B) For the first simplification, we grow the basis size iteratively. (C) For the second simplification, we split the basis in symmetry sectors, labelled by $t \in \{0, \dots, m\}$.

where we have lightened the notation and now simply assume that \mathbf{a} is a bitstring associated to a parent, and \mathbf{b} with a child. We also have that $H_{d-1}^{(0)} \equiv 1$. After p iterations, only the local fields and the edge between the two roots (labelled by 1 and 2) of the 2-tree remain, so finally we have that

$$\langle \gamma, \beta | Z_1 Z_2 | \gamma, \beta \rangle^{2\text{-tree}} = \sum_{\mathbf{z}_1 \mathbf{z}_2} z_1^{[0]} z_2^{[0]} f(\mathbf{z}_1) f(\mathbf{z}_2) H_{d-1}^{(p)}(\mathbf{z}_1) H_{d-1}^{(p)}(\mathbf{z}_2) \exp\left(i \frac{1}{\sqrt{d}} \mathbf{\Gamma} \cdot \mathbf{z}_1 \mathbf{z}_2\right) \exp\left(i \frac{h}{\sqrt{d}} \mathbf{\Gamma} \cdot (\mathbf{z}_1 + \mathbf{z}_2)\right). \quad (\text{A17})$$

For the 1-tree, the procedure is exactly the same. However, the root (labelled by 1) has now d equivalent branches. Therefore, the final iteration needs to be modified to

$$H_d^{(p)}(\mathbf{a}) = \left[\sum_{\mathbf{b}} f(\mathbf{b}) H_{d-1}^{(p-1)}(\mathbf{b}) \exp\left(i \frac{1}{\sqrt{d}} \mathbf{\Gamma} \cdot \mathbf{a} \mathbf{b}\right) \exp\left(i \frac{h}{\sqrt{d}} \mathbf{\Gamma} \cdot \mathbf{b}\right) \right]^d. \quad (\text{A18})$$

The earlier iterations remain unchanged. Therefore, the local expectation value becomes

$$\langle \gamma, \beta | Z_1 | \gamma, \beta \rangle^{1\text{-tree}} = \sum_{\mathbf{z}_1} z_1^{[0]} f(\mathbf{z}_1) H_d^{(p)}(\mathbf{z}_1) \exp\left(i \frac{h}{\sqrt{d}} \mathbf{\Gamma} \cdot \mathbf{z}_1\right). \quad (\text{A19})$$

The time complexity is the same for every step in the recursion in this case. Therefore the overall time complexity for the evaluation of the energy density [see Eq. (4)] is $O((p+1)2^{4p+2})$. As a difference with Ref. [19], note that $H_d^{(m)}(\mathbf{a})$ is generally not real anymore. This is a consequence of the breaking of the \mathbb{Z}_2 symmetry if $h \neq 0$.

2. First speed-up: Expanding the basis size at every iteration

In the last section, we wrote down similar expressions as in Ref. [19], however with a local field included. In this section, we will discuss a first speed-up of this iterative procedure. Up to now, we did not take into account the explicit angle dependencies, that can be seen in Fig. 1(C). Taking this into account does, of course, not alter the final result, as unitary cancellations are implicit. However, taking into account this dependence explicitly means that, for example, $H_{d-1}^{(1)}(\mathbf{a})$ should only depend on γ_1 , $H_{d-1}^{(2)}(\mathbf{a})$ only on $\gamma_1, \gamma_2, \beta_1$, and so on. This is however not the case in Eq. (A16), but can be easily imposed yielding more compact iterations. We start by imposing the independence in Eq. (A15), this gives

$$H_{d-1}^{(1)}(\mathbf{a}) \rightarrow H_{d-1}^{(1)}(\mathbf{a}^{(1)}) = \left[\cos\left(\frac{1}{\sqrt{d}} \mathbf{\Gamma}^{(1)} \cdot \mathbf{a}^{(1)}\right) \right]^{d-1} = \left[\cos\left(\frac{\gamma_1}{\sqrt{d}} (a_1 - a_{-1})\right) \right]^{d-1} \quad (\text{A20})$$

where we define the vectors of length $2m$

$$\mathbf{\Gamma}^{(m)} = (\gamma_1, \dots, \gamma_m, -\gamma_m, \dots, -\gamma_1), \quad (\text{A21})$$

and (to unify the notation with the QAOA angles, the subscripts now relate to the QAOA depth)

$$\mathbf{a}^{(m)} = (a_1, \dots, a_m, a_{-m}, \dots, a_{-1}), \quad a_i \in \{-1, 1\}. \quad (\text{A22})$$

Doing the same in the general case $H_{d-1}^{(m)}(\mathbf{a}) \rightarrow H_{d-1}^{(m)}(\mathbf{a}^{(m)})$ gives

$$H_{d-1}^{(m)}(\mathbf{a}^{(m)}) = \left[\sum_{\mathbf{b}^{(m-1)}} g(\mathbf{b}^{(m-1)}) H_{d-1}^{(m-1)}(\mathbf{b}^{(m-1)}) \exp\left(i \frac{1}{\sqrt{d}} \mathbf{\Gamma}^{(m-1)} \cdot \mathbf{a}^{(m-1)} \mathbf{b}^{(m-1)}\right) \exp\left(i \frac{h}{\sqrt{d}} \mathbf{\Gamma}^{(m-1)} \cdot \mathbf{b}^{(m-1)}\right) \right] \quad (\text{A23})$$

$$\frac{1}{2} \left(\langle b_{m-1} | e^{i\beta_{m-1}X} | 1 \rangle \langle 1 | e^{-i\beta_{m-1}X} | b_{-m+1} \rangle \exp\left(i \frac{\gamma_m}{\sqrt{d}} (a_m - a_{-m})\right) \right) \quad (\text{A24})$$

$$+ \langle b_{m-1} | e^{i\beta_{m-1}X} | -1 \rangle \langle -1 | e^{-i\beta_{m-1}X} | b_{-m+1} \rangle \exp\left(-i \frac{\gamma_m}{\sqrt{d}} (a_m - a_{-m})\right) \Big]^{d-1}. \quad (\text{A25})$$

In the last two lines, we have performed the summation over $b_m = b_{-m}$ explicitly. The function with reduced beta dependences is now defined as

$$g(\mathbf{b}^{(m-1)}) = \langle b_1 | e^{i\beta_1 X} | b_2 \rangle \dots \langle b_{m-2} | e^{i\beta_{m-2} X} | b_{m-1} \rangle \langle b_{-(m-1)} | e^{-i\beta_{m-2} X} | b_{-(m-2)} \rangle \dots \langle b_{-2} | e^{-i\beta_1 X} | b_{-1} \rangle. \quad (\text{A26})$$

This follows from the elimination of spurious variables in $f(\mathbf{b})$

$$\sum_{\substack{b_{m+1} \dots b_p b_0 \\ b_{-p} \dots b_{-(m-1)}}} f(\mathbf{b}) = \frac{1}{2} \sum_{\substack{b_{m+1} \dots b_p b_0 \\ b_{-p} \dots b_{-(m-1)}}} \langle b_1 | e^{i\beta_1 X} | b_2 \rangle \langle b_2 | e^{i\beta_2 X} | b_3 \rangle \dots \langle b_p | e^{i\beta_p X} | b_0 \rangle \quad (\text{A27})$$

$$\langle b_0 | e^{-i\beta_p X} | b_{-p} \rangle \dots \langle b_{-3} | e^{-i\beta_2 X} | b_{-2} \rangle \langle b_{-2} | e^{-i\beta_1 X} | b_{-1} \rangle \quad (\text{A28})$$

$$= \frac{1}{2} \langle b_1 | e^{i\beta_1 X} | b_2 \rangle \dots \langle b_{m-1} | e^{i\beta_{m-1} X} | b_m \rangle \langle b_m | b_{-m} \rangle \quad (\text{A29})$$

$$\langle b_{-m} | e^{-i\beta_{m-1} X} | b_{-(m-1)} \rangle \dots \langle b_{-2} | e^{-i\beta_1 X} | b_{-1} \rangle \quad (\text{A30})$$

$$= \frac{1}{2} g(\mathbf{b}^{(m-1)}) \langle b_{m-1} | e^{i\beta_{m-1} X} | b_m \rangle \langle b_m | e^{-i\beta_{m-1} X} | b_{-(m-1)} \rangle. \quad (\text{A31})$$

Then the final result can be modified to

$$\langle \gamma, \beta | Z_1 Z_2 | \gamma, \beta \rangle^{2\text{-tree}} = \quad (\text{A32})$$

$$\sum_{\mathbf{a}^{(p)} \mathbf{b}^{(p)}} g(\mathbf{a}^{(p-1)}) g(\mathbf{b}^{(p-1)}) H_{d-1}^{(p)}(\mathbf{a}^{(p)}) H_{d-1}^{(p)}(\mathbf{b}^{(p)}) \exp\left(i \frac{1}{\sqrt{d}} \mathbf{\Gamma} \cdot \mathbf{a}^{(p)} \mathbf{b}^{(p)}\right) \exp\left(i \frac{h}{\sqrt{d}} \mathbf{\Gamma} \cdot (\mathbf{a}^{(p)} + \mathbf{b}^{(p)})\right) \quad (\text{A33})$$

$$\sum_{a_0 b_0} \frac{a_0 b_0}{4} \langle a_p | e^{i\beta_p X} | a_0 \rangle \langle a_0 | e^{-i\beta_p X} | a_{-p} \rangle \langle b_p | e^{i\beta_p X} | b_0 \rangle \langle b_0 | e^{-i\beta_p X} | b_{-p} \rangle. \quad (\text{A34})$$

The summation over a_0 and b_0 can be worked out, reducing the scaling by a prefactor to $O(2^{4p})$. The onsite term simplified in this way becomes

$$\langle \gamma, \beta | Z_1 | \gamma, \beta \rangle^{1\text{-tree}} = \sum_{\mathbf{a}^{(p)}} g(\mathbf{a}^{(p-1)}) H_{d-1}^{(p)}(\mathbf{a}^{(p)}) \exp\left(i \frac{h}{\sqrt{d}} \mathbf{\Gamma} \cdot \mathbf{a}^{(p)}\right) \sum_{a_0} \frac{a_0}{2} \langle a_p | e^{i\beta_p X} | a_0 \rangle \langle a_0 | e^{-i\beta_p X} | a_{-p} \rangle. \quad (\text{A35})$$

3. Second speed-up: Decomposing the basis into T-symmetric blocks

In this section, we discuss our last speed-up that is related to a splitting of the basis in blocks that carry a symmetry label. Some properties of these been discussed in the Appendix of Ref. [19], with as goal providing simpler iterations in the $d \rightarrow \infty$ limit, but remain unexploited for the finite d iteration. To every bitstring of the form $\mathbf{a}^{(m)}$ [see Eq. (A22)], we can associate a symmetry label $t \in \{0, 1, \dots, m\}$, $\mathbf{a}^{(m)} \rightarrow \mathbf{a}_t^{(m)}$ that characterizes how reflection symmetric the bitstring is, i.e. when $t = 0$ the bitstring is completely symmetric, when $t = m$ it is not symmetric. This is summarized

t	# bitstrings	bitstring
0	2^m	$\mathbf{a}_0^{(m)} = (a_1, \dots, a_{m-1}, a_m, a_m, a_{m-1}, \dots, a_1)$
1	2^m	$\mathbf{a}_1^{(m)} = (a_1, \dots, a_{m-1}, a_m, a_m, a_{m-1}, \dots, -a_1)$
2	2^{m+1}	$\mathbf{a}_2^{(m)} = (a_1, a_2, \dots, a_{m-1}, a_m, a_m, a_{m-1}, \dots, -a_2, a_{-1})$
\vdots	\vdots	\vdots
m	2^{2m-1}	$\mathbf{a}_m^{(m)} = (a_1, \dots, a_{m-1}, a_m, -a_m, a_{-(m-1)}, \dots, a_{-1})$

TABLE III. Labelling of the basis $\{\mathbf{a}^{(m)}\}$, $|\{\mathbf{a}^{(m)}\}| = 2^{2m}$, according to t .

in Table A3. This label characterizes the fixed points in the iterative procedure. This is the most straightforward to see for $t = 0$, where we have that $H_d^{(m)}(\mathbf{a}_0^{(m)}) = 1, \forall m$. We can show this by induction. From Eq. (A20) we see that this is indeed true for $m = 1$. Assuming that this is true at level $m - 1$, we have for level m [see Eq. (A23)]

$$H_{d-1}^{(m)}(\mathbf{a}_0^{(m)}) = \left[\sum_{\mathbf{b}^{(m-1)}} g(\mathbf{b}^{(m-1)}) \frac{1}{2} \langle b_{m-1} | b_{-(m-1)} \rangle \exp\left(i \frac{1}{\sqrt{d}} \mathbf{\Gamma}^{(m-1)} \cdot \mathbf{a}_0^{(m-1)} \mathbf{b}^{(m-1)}\right) \exp\left(i \frac{h}{\sqrt{d}} \mathbf{\Gamma}^{(m-1)} \cdot \mathbf{b}^{(m-1)}\right) \right]^{d-1} \quad (\text{A36})$$

$$= \dots = \left[\sum_{b_1, b_{-1}} \frac{1}{2} \langle b_1 | b_{-1} \rangle \exp\left(i \frac{1}{\sqrt{d}} \gamma_1 a_1 (b_1 - b_{-1})\right) \exp\left(i \frac{h}{\sqrt{d}} \gamma_1 (b_1 - b_{-1})\right) \right]^{d-1} = 1. \quad (\text{A37})$$

Similarly, if $t < m$ we have that $H_d^{(m)}(\mathbf{a}_t^{(m)}) = H_d^{(t)}(\mathbf{a}_t^{(t)})$. Here $\mathbf{a}^{(t)}$ is obtained from $\mathbf{a}^{(m)}$ by pruning away the symmetric bits, i.e.

$$\mathbf{a}_t^{(m)} = (a_1, \dots, a_t, a_{t+1}, \dots, a_m, a_m, \dots, a_{t+1}, -a_t, \dots, a_{-1}) \quad (\text{A38})$$

$$\rightarrow \mathbf{a}_t^{(t)} = (a_1, \dots, a_t, -a_t, \dots, a_{-1}). \quad (\text{A39})$$

The proof is similar as before, indeed, from Eq. (A23) we can immediately see that a sequence of simplifications is entered when $a_m = a_{-m}$. This means that at each iteration level m , we ‘only’ need to evaluate the 2^{2m-1} bitstrings that have $t = m$.

We can reduce this further by a factor of two by realizing that $H_{d-1}^{(m)}(R(\mathbf{a}_m^{(m)})) = [H_{d-1}^{(m)}(\mathbf{a}_m^{(m)})]^*$, where R is the reflection operator

$$R : (a_1, \dots, a_m, -a_m, \dots, a_{-1}) \rightarrow (a_{-1}, \dots, -a_t, a_t, \dots, a_1). \quad (\text{A40})$$

Now, we can work out the final contraction taking into account the symmetry sectors

$$\langle \boldsymbol{\gamma}, \boldsymbol{\beta} | Z_1 Z_2 | \boldsymbol{\gamma}, \boldsymbol{\beta} \rangle^{2\text{-tree}} = \sum_{t=1}^p \sum_{\mathbf{a}_t^{(t)} \mathbf{b}_t^{(t)}} G_t(a_t) G_t(b_t) g(\mathbf{a}_t^{(t-1)}) g(\mathbf{b}_t^{(t-1)}) H_{d-1}^{(t)}(\mathbf{a}_t^{(t)}) H_{d-1}^{(t)}(\mathbf{b}_t^{(t)}) \quad (\text{A41})$$

$$\exp\left(i \mathbf{\Gamma}^{(t)} \cdot \left(\frac{\mathbf{a}_t^{(t)} \mathbf{b}_t^{(t)} + h(\mathbf{a}_t^{(t)} + \mathbf{b}_t^{(t)})}{\sqrt{d}} \right)\right) \quad (\text{A42})$$

$$+ 2 \sum_{t_a > t_b} \sum_{\mathbf{a}_{t_a}^{(t_a)} \mathbf{b}_{t_b}^{(t_a)}} G(a_{t_a}) \tilde{G}(b_{t_b}) g(\mathbf{a}_{t_a}^{(t_a-1)}) g(\mathbf{b}_{t_b}^{(t_a-1)}) H_{d-1}^{(t_a)}(\mathbf{a}_{t_a}^{(t_a)}) H_{d-1}^{(t_b)}(\mathbf{b}_{t_b}^{(t_b)}) \quad (\text{A43})$$

$$\exp\left(i \mathbf{\Gamma}^{(t_a)} \cdot \left(\frac{\mathbf{a}_{t_a}^{(t_a)} \mathbf{b}_{t_b}^{(t_a)} + h(\mathbf{a}_{t_a}^{(t_a)} + \mathbf{b}_{t_b}^{(t_a)})}{\sqrt{d}} \right)\right). \quad (\text{A44})$$

Here $G(a_t) \equiv G(a_t; \beta_t, \dots, \beta_p)$ results from the elimination of spurious symmetric variables

$$G(a_t) = \sum_{a_{t+1}, \dots, a_p, a_0} \frac{a_0}{2} \langle a_t | e^{i\beta_t X} | a_{t+1} \rangle \langle a_{t+1} | e^{-i\beta_t X} | -a_t \rangle | \langle a_{t+1} | e^{i\beta_{t+1} X} | a_{t+2} \rangle |^2 \dots | \langle a_p | e^{i\beta_p X} | a_0 \rangle |^2 \quad (\text{A45})$$

$$= -\frac{a_t}{2} i \sin(2\beta_t) \cos(2\beta_{t+1}) \dots \cos(2\beta_p). \quad (\text{A46})$$

Notice that if $t = p$, we have that $G(a_p) = -\frac{a_p}{2}i \sin(2\beta_p)$, and similarly,

$$\tilde{G}(a_t) = \sum_{a_{t+1}, \dots, a_p, a_0} \frac{a_0}{2} |\langle a_t | e^{i\beta_t X} | a_{t+1} \rangle|^2 |\langle a_{t+1} | e^{i\beta_{t+1} X} | a_{t+2} \rangle|^2 \dots |\langle a_p | e^{i\beta_p X} | a_0 \rangle|^2 \quad (\text{A47})$$

$$= \frac{a_t}{2} \cos(2\beta_t) \cos(2\beta_{t+1}) \dots \cos(2\beta_p). \quad (\text{A48})$$

For the onsite term, applying the same procedure yields

$$\langle \gamma, \beta | Z_1 | \gamma, \beta \rangle^{1\text{-tree}} = \sum_{t=1}^p \sum_{\mathbf{a}_t} G_t(a_t) g(\mathbf{a}_t^{(t-1)}) H_{d-1}^{(t)}(\mathbf{a}_t^{(t)}) \exp\left(i \frac{h}{\sqrt{d}} \mathbf{\Gamma}^{(t)} \cdot \mathbf{a}_t^{(t)}\right) \quad (\text{A49})$$

$$(\text{A50})$$

4. The performance of tree QAOA for large regularity

In this section, we investigate the performance of tree QAOA in the large d limit with fixed p . We focus on the case $p = 1$ explicitly, but expect a similar behavior for $p > 1$. From the previous section, we can easily reduce the expectation values to $p = 1$, this gives

$$\langle \gamma, \beta | Z_1 Z_2 | \gamma, \beta \rangle^{2\text{-tree}} = -\frac{1}{2} [\sin(2\beta)]^2 \left[\cos\left(\frac{4h\gamma}{\sqrt{d}}\right) - 1 \right] \left[\cos\left(\frac{2\gamma}{\sqrt{d}}\right) \right]^{2d-2} \quad (\text{A51})$$

$$+ \sin(4\beta) \sin\left(\frac{2\gamma}{\sqrt{d}}\right) \cos\left(\frac{2h\gamma}{\sqrt{d}}\right) \left[\cos\left(\frac{2\gamma}{\sqrt{d}}\right) \right]^{d-1} \quad (\text{A52})$$

where the two terms correspond to the two summations in Eq. (A41), more precisely the cases where $t_a = t_b = 1$ and $t_a = 1, t_b = 0$). The local term becomes

$$\langle \gamma, \beta | Z_1 | \gamma, \beta \rangle^{1\text{-tree}} = \sin(2\beta) \sin\left(\frac{2h\gamma}{\sqrt{d}}\right) \left[\cos\left(\frac{2\gamma}{\sqrt{d}}\right) \right]^d, \quad (\text{A53})$$

which is just the single case $t_a = 1$ in Eq. (A49).

The $p = 1$ tree QAOA aims to minimize Eq. (4), i.e. the following function

$$\frac{h}{\sqrt{d}} \langle \gamma, \beta | Z_1 | \gamma, \beta \rangle^{1\text{-tree}} + \frac{\sqrt{d}}{2} \langle \gamma, \beta | Z_1 Z_2 | \gamma, \beta \rangle^{2\text{-tree}} = \frac{h}{\sqrt{d}} \sin(2\beta) \sin\left(\frac{2h\gamma}{\sqrt{d}}\right) \left[\cos\left(\frac{2\gamma}{\sqrt{d}}\right) \right]^d + \quad (\text{A54})$$

$$\frac{\sqrt{d}}{2} \left\{ -\frac{1}{2} [\sin(2\beta)]^2 \left[\cos\left(\frac{4h\gamma}{\sqrt{d}}\right) - 1 \right] \left[\cos\left(\frac{2\gamma}{\sqrt{d}}\right) \right]^{2d-2} + \sin(4\beta) \sin\left(\frac{2\gamma}{\sqrt{d}}\right) \cos\left(\frac{2h\gamma}{\sqrt{d}}\right) \left[\cos\left(\frac{2\gamma}{\sqrt{d}}\right) \right]^{d-1} \right\}. \quad (\text{A55})$$

In case of MaxCut, $h = 0$, trivially $\langle \gamma, \beta | Z_1 | \gamma, \beta \rangle^{1\text{-tree}} = 0$. In this case, it can be seen that the two-body term $\langle \gamma, \beta | Z_1 Z_2 | \gamma, \beta \rangle^{2\text{-tree}}$ is minimized by choosing $\beta = -\pi/8$, irrespective of d . Upon increasing d , we then expect the optimal γ to vanish, such that $\langle \gamma, \beta | Z_1 Z_2 | \gamma, \beta \rangle^{2\text{-tree}} \rightarrow 0$. In this limit the cut fraction obtained by tree QAOA is $1/2$. This is the same as random guessing, which is optimal in this limit. Therefore the MaxCut approximation ratio also converges to 1.

In case of MIS, $h \approx d$, the single-body term $\langle \gamma, \beta | Z_1 | \gamma, \beta \rangle^{1\text{-tree}}$ contributes. For increasing d , we have that $\beta \rightarrow -\pi/4$ and $\gamma \rightarrow \frac{\pi}{4\sqrt{d}}$. This means that in this limit $\langle \gamma, \beta | Z_1 Z_2 | \gamma, \beta \rangle^{2\text{-tree}} \rightarrow 1$ and $\langle \gamma, \beta | Z_1 | \gamma, \beta \rangle^{1\text{-tree}} \rightarrow -1$. Then, we have a vanishing independence ratio, and thus a vanishing MIS approximation ratio.

Appendix B: Tree angles for MaxCut and MIS

We include the tree angles that were used in the finite-size simulations shown in Fig. 6 in the tables below. The angles below are obtained for the QAOA ansatz given in Eq. (2), for better table alignment we however show $\beta \rightarrow -\beta$. For MaxCut these angles are found by taking $h = 0$, and $h = 2$ for MIS.

QAOA depth p	Tree angles for MaxCut $d = 3$
1	$\gamma = (0.5330)$ $\beta = (0.3927)$
2	$\gamma = (0.4225, 0.7776)$ $\beta = (0.5549, 0.2924)$
3	$\gamma = (0.3653, 0.6914, 0.8114)$ $\beta = (0.6090, 0.4596, 0.2357)$
4	$\gamma = (0.3540, 0.6760, 0.8557, 1.0019)$ $\beta = (0.5996, 0.4343, 0.2968, 0.1590)$
5	$\gamma = (0.3111, 0.6115, 0.7119, 0.8697, 0.9993)$ $\beta = (0.6317, 0.5225, 0.3901, 0.2760, 0.1493)$
6	$\gamma = (0.2870, 0.5591, 0.6336, 0.7248, 0.8749, 0.9763)$ $\beta = (0.6359, 0.5344, 0.4633, 0.3600, 0.2585, 0.1388)$
7	$\gamma = (0.2682, 0.5342, 0.5960, 0.6496, 0.7426, 0.8845, 0.9750)$ $\beta = (0.6476, 0.5531, 0.4893, 0.4448, 0.3408, 0.2444, 0.1312)$
8	$\gamma = (0.2537, 0.5076, 0.5674, 0.6132, 0.6619, 0.7490, 0.8892, 0.9669)$ $\beta = (0.6492, 0.5555, 0.5013, 0.4690, 0.4202, 0.3195, 0.2310, 0.1229)$

QAOA depth p	Tree angles for MaxCut $d = 4$
1	$\gamma = (0.5236)$ $\beta = (0.3927)$
2	$\gamma = (0.4078, 0.7397)$ $\beta = (0.5341, 0.2830)$
3	$\gamma = (0.3545, 0.6514, 0.7543)$ $\beta = (0.5879, 0.4232, 0.2230)$
4	$\gamma = (0.3150, 0.5876, 0.6732, 0.7712)$ $\beta = (0.6050, 0.4778, 0.3613, 0.1875)$
5	$\gamma = (0.2909, 0.5468, 0.6033, 0.6872, 0.7844)$ $\beta = (0.6225, 0.5051, 0.4167, 0.3253, 0.1628)$
6	$\gamma = (0.2687, 0.5128, 0.5636, 0.6141, 0.6957, 0.7867)$ $\beta = (0.6293, 0.5232, 0.4528, 0.3883, 0.2981, 0.1459)$
7	$\gamma = (0.2537, 0.4890, 0.5317, 0.5757, 0.6214, 0.6976, 0.7885)$ $\beta = (0.6378, 0.5327, 0.4719, 0.4325, 0.3632, 0.2778, 0.1339)$
8	$\gamma = (0.2405, 0.4690, 0.5113, 0.5480, 0.5851, 0.6257, 0.7221, 0.8339)$ $\beta = (0.6405, 0.5385, 0.4817, 0.4526, 0.4101, 0.3452, 0.2605, 0.1198)$

QAOA depth p	Tree angles for MIS $d = 3$
1	$\gamma = (0.4299)$ $\beta = (0.3986)$
2	$\gamma = (0.3678, 0.7957)$ $\beta = (0.5175, 0.2642)$
3	$\gamma = (0.3260, 0.6720, 0.7582)$ $\beta = (0.5777, 0.3680, 0.2103)$
4	$\gamma = (0.2846, 0.6045, 0.7105, 0.7419)$ $\beta = (0.6046, 0.4686, 0.3396, 0.1846)$
5	$\gamma = (0.2722, 0.5640, 0.6536, 0.7082, 0.7908)$ $\beta = (0.6174, 0.4776, 0.4222, 0.3088, 0.1525)$
6	$\gamma = (0.2537, 0.5324, 0.6102, 0.6370, 0.7164, 0.7872)$ $\beta = (0.6350, 0.5082, 0.4523, 0.4136, 0.2866, 0.1533)$
7	$\gamma = (0.2316, 0.4843, 0.5687, 0.5937, 0.6238, 0.7266, 0.7577)$ $\beta = (0.6337, 0.5026, 0.4636, 0.4304, 0.3718, 0.2725, 0.1410)$
8	$\gamma = (0.2249, 0.4734, 0.5590, 0.5833, 0.6082, 0.6697, 0.7368, 0.7882)$ $\beta = (0.6428, 0.5181, 0.4779, 0.4519, 0.3974, 0.3589, 0.2566, 0.1203)$

QAOA depth p	Tree angles for MIS $d = 4$
1	$\gamma = (0.3376)$ $\beta = (0.4240)$
2	$\gamma = (0.3123, 0.8352)$ $\beta = (0.5169, 0.2407)$
3	$\gamma = (0.2756, 0.6606, 0.7660)$ $\beta = (0.5628, 0.3024, 0.1942)$
4	$\gamma = (0.2405, 0.5462, 0.6808, 0.6781)$ $\beta = (0.5745, 0.3541, 0.2618, 0.1563)$
5	$\gamma = (0.2245, 0.5178, 0.6307, 0.6445, 0.6808)$ $\beta = (0.6138, 0.4152, 0.3412, 0.2583, 0.1410)$
6	$\gamma = (0.2043, 0.4545, 0.5887, 0.6121, 0.6307, 0.7054)$ $\beta = (0.6162, 0.4200, 0.3845, 0.3231, 0.2229, 0.1152)$
7	$\gamma = (0.1981, 0.4406, 0.5595, 0.5777, 0.5887, 0.6775, 0.7116)$ $\beta = (0.6350, 0.4475, 0.4108, 0.3828, 0.3036, 0.1984, 0.1188)$
8	$\gamma = (0.1765, 0.3840, 0.5239, 0.5596, 0.5595, 0.6197, 0.6817, 0.6833)$ $\beta = (0.6278, 0.4452, 0.4267, 0.3991, 0.3570, 0.2689, 0.1946, 0.1085)$

-
- [1] R. P. Feynman, *International Journal of Theoretical Physics* **21**, 467–488 (1982).
- [2] J. I. Cirac and P. Zoller, *Nature Physics* **8**, 264–266 (2012).
- [3] I. M. Georgescu, S. Ashhab, and F. Nori, *Rev. Mod. Phys.* **86**, 153 (2014).
- [4] A. W. Harrow, A. Hassidim, and S. Lloyd, *Phys. Rev. Lett.* **103**, 150502 (2009).
- [5] Y. Liu, S. Arunachalam, and K. Temme, *Nature Physics* **17**, 1013–1017 (2021).
- [6] H.-Y. Huang, R. Kueng, and J. Preskill, *Phys. Rev. Lett.* **126**, 190505 (2021).
- [7] R. Sweke, J.-P. Seifert, D. Hangleiter, and J. Eisert, *Quantum* **5**, 417 (2021).
- [8] L. K. Grover, (1996), [arXiv:quant-ph/9605043](https://arxiv.org/abs/quant-ph/9605043).
- [9] A. Abbas, A. Ambainis, B. Augustino, A. Bäertschi, H. Buhrman, C. Coffrin, G. Cortiana, V. Dunjko, D. J. Egger, B. G. Elmegreen, N. Franco, F. Fratini, B. Fuller, J. Gacon, C. Gondiulea, S. Gribling, S. Gupta, S. Hadfield, R. Heese, G. Kircher, T. Kleinert, T. Koch, G. Korpas, S. Lenk, J. Marecek, V. Markov, G. Mazzola, S. Mensa, N. Mohseni, G. Nannicini, C. O’Meara, E. P. Tapia, S. Pokutta, M. Proissl, P. Rebentrost, E. Sahin, B. C. B. Symons, S. Tornow, V. Valls, S. Woerner, M. L. Wolf-Bauwens, J. Yard, S. Yarkoni, D. Zechiel, S. Zhuk, and C. Zoufal, (2023), [10.48550/ARXIV.2312.02279](https://arxiv.org/abs/10.48550/ARXIV.2312.02279), [arXiv:2312.02279](https://arxiv.org/abs/2312.02279) [quant-ph].
- [10] J. Preskill, *Quantum* **2**, 79 (2018) **2**, 79 (2018), [arXiv:1801.00862](https://arxiv.org/abs/1801.00862) [quant-ph].
- [11] E. Farhi, J. Goldstone, and S. Gutmann, (2014), [10.48550/ARXIV.1411.4028](https://arxiv.org/abs/10.48550/ARXIV.1411.4028), [arXiv:1411.4028](https://arxiv.org/abs/1411.4028) [quant-ph].
- [12] E. Farhi, J. Goldstone, and S. Gutmann, (2014), [10.48550/ARXIV.1412.6062](https://arxiv.org/abs/10.48550/ARXIV.1412.6062), [arXiv:1412.6062](https://arxiv.org/abs/1412.6062) [quant-ph].
- [13] E. Farhi and A. W. Harrow, (2016), [10.48550/ARXIV.1602.07674](https://arxiv.org/abs/10.48550/ARXIV.1602.07674), [arXiv:1602.07674](https://arxiv.org/abs/1602.07674) [quant-ph].
- [14] S. Hadfield, Z. Wang, B. O’Gorman, E. G. Rieffel, D. Venturelli, and R. Biswas, *Algorithms* **12.2** (2019): 34. (Special issue “Quantum Optimization Theory, Algorithms, and Applications”) **12**, 34 (2017), [arXiv:1709.03489](https://arxiv.org/abs/1709.03489) [quant-ph].
- [15] E. Zahedinejad and A. Zaribafiyani, (2017), [10.48550/ARXIV.1708.05294](https://arxiv.org/abs/10.48550/ARXIV.1708.05294), [arXiv:1708.05294](https://arxiv.org/abs/1708.05294) [quant-ph].
- [16] Z. Wang, S. Hadfield, Z. Jiang, and E. G. Rieffel, *Phys. Rev. A* **97**, 022304 (2018).
- [17] K. Blekos, D. Brand, A. Ceschini, C.-H. Chou, R.-H. Li, K. Pandya, and A. Summer, *Physics Reports* **1068**, 1 (2023), [arXiv:2306.09198](https://arxiv.org/abs/2306.09198) [quant-ph].
- [18] E. Makover and J. McGowan, “Regular trees in random regular graphs,” (2006).
- [19] J. Basso, E. Farhi, K. Marwaha, B. Villalonga, and L. Zhou, In *Proceedings of the 17th Conference on the Theory of Quantum Computation, Communication and Cryptography (TQC ’22)*, 7:1–7:21, (2022) (2021), [10.4230/LIPICS.TQC.2022.7](https://arxiv.org/abs/10.4230/LIPICS.TQC.2022.7), [arXiv:2110.14206](https://arxiv.org/abs/2110.14206) [quant-ph].
- [20] F. G. S. L. Brandao, M. Broughton, E. Farhi, S. Gutmann, and H. Neven, (2018), [10.48550/ARXIV.1812.04170](https://arxiv.org/abs/10.48550/ARXIV.1812.04170), [arXiv:1812.04170](https://arxiv.org/abs/1812.04170) [quant-ph].
- [21] M. Streif and M. Leib, *Quantum Science and Technology* **5**, 034008 (2020).
- [22] A. Galda, X. Liu, D. Lykov, Y. Alexeev, and I. Safro, (2021), [10.48550/ARXIV.2106.07531](https://arxiv.org/abs/10.48550/ARXIV.2106.07531), [arXiv:2106.07531](https://arxiv.org/abs/2106.07531) [quant-ph].
- [23] A. Galda, E. Gupta, J. Falla, X. Liu, D. Lykov, Y. Alexeev, and I. Safro, (2023), [10.48550/ARXIV.2307.05420](https://arxiv.org/abs/10.48550/ARXIV.2307.05420), [arXiv:2307.05420](https://arxiv.org/abs/2307.05420) [quant-ph].
- [24] G. E. Crooks, (2018), [10.48550/ARXIV.1811.08419](https://arxiv.org/abs/10.48550/ARXIV.1811.08419), [arXiv:1811.08419](https://arxiv.org/abs/1811.08419) [quant-ph].
- [25] J. Wurtz and P. J. Love, *Phys. Rev. A* **103**, 042612 (2021) **103**, 042612 (2020), [arXiv:2010.11209](https://arxiv.org/abs/2010.11209) [quant-ph].
- [26] J. Wurtz and D. Lykov, *Phys. Rev. A* **104**, 052419 (2021).
- [27] B. Barak and K. Marwaha, *13th Innovations in Theoretical Computer Science Conference (ITCS 2022)*; Article No. 14 (2021), [10.4230/LIPICS.ITCS.2022.14](https://arxiv.org/abs/10.4230/LIPICS.ITCS.2022.14), [arXiv:2106.05900](https://arxiv.org/abs/2106.05900) [quant-ph].
- [28] K. Marwaha, *Quantum* **5**, 437 (2021) **5**, 437 (2021), [arXiv:2101.05513](https://arxiv.org/abs/2101.05513) [quant-ph].
- [29] D. Lykov, J. Wurtz, C. Poole, M. Saffman, T. Noel, and Y. Alexeev, (2022), [10.48550/ARXIV.2206.03579](https://arxiv.org/abs/10.48550/ARXIV.2206.03579), [arXiv:2206.03579](https://arxiv.org/abs/2206.03579) [quant-ph].
- [30] M. X. Goemans and D. P. Williamson, *Journal of the ACM* **42**, 1115–1145 (1995).
- [31] S. Khot, G. Kindler, E. Mossel, and R. O’Donnell, *SIAM Journal on Computing* **37**, 319 (2007), <https://doi.org/10.1137/S0097539705447372>.
- [32] M. B. Hastings, (2019), [10.48550/ARXIV.1905.07047](https://arxiv.org/abs/10.48550/ARXIV.1905.07047), [arXiv:1905.07047](https://arxiv.org/abs/1905.07047) [quant-ph].
- [33] G. G. Guerreschi and A. Y. Matsuura, *Scientific Reports* **9** (2019), [10.1038/s41598-019-43176-9](https://arxiv.org/abs/10.1038/s41598-019-43176-9).
- [34] A. E. Alaoui, A. Montanari, and M. Sellke, (2021), [10.48550/ARXIV.2111.06813](https://arxiv.org/abs/10.48550/ARXIV.2111.06813), [arXiv:2111.06813](https://arxiv.org/abs/2111.06813) [math.PR].
- [35] E. Farhi, J. Goldstone, S. Gutmann, and L. Zhou, *Quantum* **6**, 759 (2022).
- [36] S. Boulebnane and A. Montanaro, (2021), [10.48550/ARXIV.2110.10685](https://arxiv.org/abs/10.48550/ARXIV.2110.10685), [arXiv:2110.10685](https://arxiv.org/abs/2110.10685) [quant-ph].
- [37] E. Farhi, D. Gamarnik, and S. Gutmann, (2020), [10.48550/ARXIV.2004.09002](https://arxiv.org/abs/10.48550/ARXIV.2004.09002), [arXiv:2004.09002](https://arxiv.org/abs/2004.09002) [quant-ph].
- [38] E. Farhi, D. Gamarnik, and S. Gutmann, (2020), [10.48550/ARXIV.2005.08747](https://arxiv.org/abs/10.48550/ARXIV.2005.08747), [arXiv:2005.08747](https://arxiv.org/abs/2005.08747) [quant-ph].
- [39] M. Mézard, T. Mora, and R. Zecchina, *Phys. Rev. Lett.* **94**, 197205 (2005).
- [40] D. Achlioptas, A. Coja-Oghlan, and F. Ricci-Tersenghi, *Random Structures & Algorithms* **38**, 251 (2011), <https://onlinelibrary.wiley.com/doi/pdf/10.1002/rsa.20323>.
- [41] D. Gamarnik and A. Jagannath, (2019), [10.48550/ARXIV.1911.06943](https://arxiv.org/abs/10.48550/ARXIV.1911.06943), [arXiv:1911.06943](https://arxiv.org/abs/1911.06943) [math.PR].
- [42] D. Gamarnik, *Proceedings of the National Academy of Sciences* **118** (2021), [10.1073/pnas.2108492118](https://arxiv.org/abs/10.1073/pnas.2108492118), [arXiv:2109.14409](https://arxiv.org/abs/2109.14409) [cs.CC].
- [43] W.-K. Chen, D. Gamarnik, D. Panchenko, and M. Rahman, *Annals of Probability* 2019, Vol. 47, No. 3, 1587–1618 **47** (2017), [10.1214/18-aop1291](https://arxiv.org/abs/10.1214/18-aop1291), [arXiv:1707.05386](https://arxiv.org/abs/1707.05386) [math.PR].
- [44] A. Auffinger, W.-K. Chen, and Q. Zeng, *CPAM* **2020** (2017), [10.48550/ARXIV.1703.06872](https://arxiv.org/abs/10.48550/ARXIV.1703.06872), [arXiv:1703.06872](https://arxiv.org/abs/1703.06872) [math.PR].

- [45] C.-N. Chou, P. J. Love, J. S. Sandhu, and J. Shi, (2021), 10.48550/ARXIV.2108.06049, arXiv:2108.06049 [quant-ph].
- [46] A. Dembo, A. Montanari, and S. Sen, *Annals of Probability*, 2017, Vol 45, No. 2, 1190- 1217 **45** (2015), 10.1214/15-aop1084, arXiv:1503.03923 [math.PR].
- [47] A. Coja-Oghlan, P. Loick, B. F. Mezei, and G. B. Sorkin, (2020), 10.48550/ARXIV.2009.10483, arXiv:2009.10483 [math.CO].
- [48] B. D. McKay, *Ars Combinatoria*, 23A 179-185. (1987).
- [49] J. Balogh, A. Kostochka, and X. Liu, (2017), 10.48550/ARXIV.1708.03996, arXiv:1708.03996 [math.CO].
- [50] D. Gamarnik and M. Sudan, (2013), 10.48550/ARXIV.1304.1831, arXiv:1304.1831 [math.PR].
- [51] S. Bravyi, A. Kliesch, R. Koenig, and E. Tang, *Phys. Rev. Lett.* 125, 260505 (2020) **125**, 260505 (2019), arXiv:1910.08980 [quant-ph].
- [52] E. Bae and S. Lee, *Quantum Information Processing* **23** (2022), 10.1007/s11128-024-04286-0, arXiv:2211.15832 [quant-ph].
- [53] Y. J. Patel, S. Jerbi, T. Bäck, and V. Dunjko, *EPJ Quantum Technol.* 11, 6 (2024) **11** (2022), 10.1140/epjqt/s40507-023-00214-w, arXiv:2207.06294 [quant-ph].
- [54] F. Wagner, J. Nüßlein, and F. Liers, (2023), 10.48550/ARXIV.2302.05493, arXiv:2302.05493 [quant-ph].
- [55] M. Dupont, B. Evert, M. J. Hodson, B. Sundar, S. Jeffrey, Y. Yamaguchi, D. Feng, F. B. Maciejewski, S. Hadfield, M. S. Alam, Z. Wang, S. Grabbe, P. A. Lott, E. G. Rieffel, D. Venturelli, and M. J. Reagor, *Science Advances* 9, 45 (2023) **9** (2023), 10.1126/sciadv.adi0487, arXiv:2303.05509 [quant-ph].
- [56] M. Dupont and B. Sundar, (2023), 10.48550/ARXIV.2307.05821, arXiv:2307.05821 [quant-ph].
- [57] J. R. Finžgar, A. Kerschbaumer, M. J. A. Schuetz, C. B. Mendl, and H. G. Katzgraber, (2023), 10.48550/ARXIV.2308.13607, arXiv:2308.13607 [quant-ph].
- [58] Z.-C. Yang, A. Rahmani, A. Shabani, H. Neven, and C. Chamon, *Physical Review X* **7**, 021027 (2017).
- [59] L. Zdeborová and S. Boettcher, *J. Stat. Mech.* (2010) P02020 **2010**, P02020 (2009), arXiv:0912.4861 [cond-mat.dis-nn].
- [60] R. Marino and S. Kirkpatrick, (2020), 10.48550/ARXIV.2003.12293, arXiv:2003.12293 [cs.DS].
- [61] M. Rahman and B. Virag, *Ann. Probab.* 45 (2017), no. 3, 1543-1577 **45** (2014), 10.1214/16-aop1094, arXiv:1402.0485 [math.PR].
- [62] A. Coja-Oghlan and C. Efthymiou, *Random Structures and Algorithms* 47 (2015) 436 - 486 **47**, 436 (2010), arXiv:1007.1378 [cs.DM].
- [63] A. S. Wein, (2020), 10.48550/ARXIV.2010.06563, arXiv:2010.06563 [cs.CC].
- [64] A. Frieze and T. Łuczak, *Journal of Combinatorial Theory, Series B* **54**, 123 (1992).
- [65] H. Hatami, L. Lovász, and B. Szegedy, (2012), 10.48550/ARXIV.1205.4356, arXiv:1205.4356 [math.CO].
- [66] A. Montanari, (2018), 10.48550/ARXIV.1812.10897, arXiv:1812.10897 [math.PR].
- [67] M. X. H. Goh, (2024), 10.48550/ARXIV.2404.06087, arXiv:2404.06087 [quant-ph].
- [68] E. Halperin, D. Livnat, and U. Zwick, *Journal of Algorithms* **53**, 169 (2004).
- [69] M. M. Hallórsson and J. Radhakrishnan, *Algorithmica* **18**, 145–163 (1997).
- [70] G. G. Guerreschi and M. Smelyanskiy, (2017), 10.48550/ARXIV.1701.01450, arXiv:1701.01450 [quant-ph].
- [71] L. Zhou, S.-T. Wang, S. Choi, H. Pichler, and M. D. Lukin, *Phys. Rev. X* 10, 021067 (2020) **10**, 021067 (2018), arXiv:1812.01041 [quant-ph].
- [72] L. Bittel and M. Kliesch, *Phys. Rev. Lett.* 127, 120502 (2021) **127**, 120502 (2021), arXiv:2101.07267 [quant-ph].